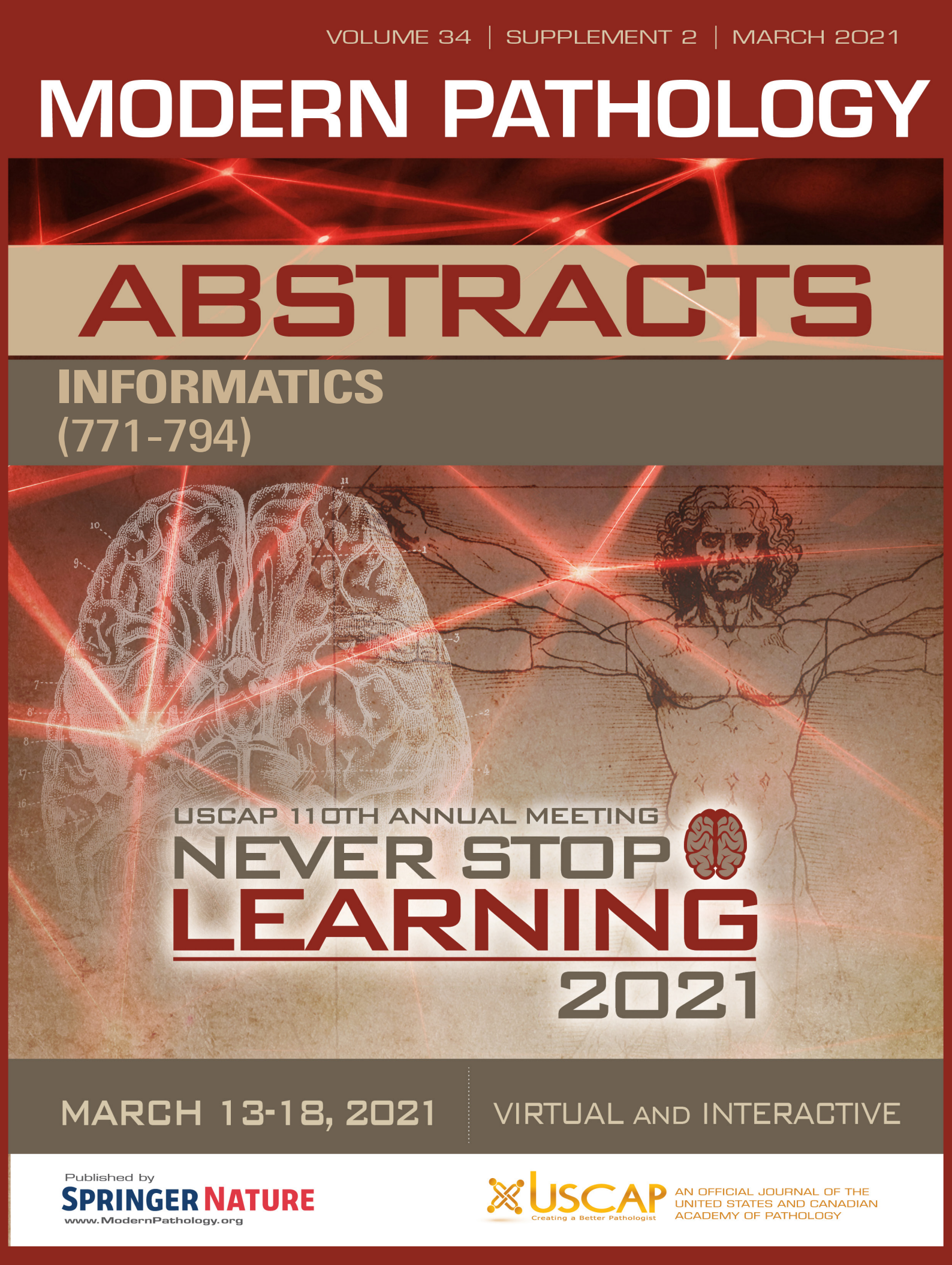


MODERN PATHOLOGY

ABSTRACTS

BONE AND SOFT TISSUE PATHOLOGY
(33-65)



USCAP 110TH ANNUAL MEETING
NEVER STOP
LEARNING
2021

MARCH 13-18, 2021

VIRTUAL AND INTERACTIVE

Published by
SPRINGER NATURE
www.ModernPathology.org

 **USCAP** AN OFFICIAL JOURNAL OF THE
UNITED STATES AND CANADIAN
ACADEMY OF PATHOLOGY
Creating a Better Pathologist

EDUCATION COMMITTEE

Jason L. Hornick
Chair

Rhonda K. Yantiss, Chair
Abstract Review Board and Assignment Committee

Kristin C. Jensen
Chair, CME Subcommittee

Laura C. Collins
Interactive Microscopy Subcommittee

Raja R. Seethala
Short Course Coordinator

Ilan Weinreb
Subcommittee for Unique Live Course Offerings

David B. Kaminsky
(Ex-Officio)
Zubair W. Baloch
Daniel J. Brat
Sarah M. Dry
William C. Faquin
Yuri Fedoriw
Karen Fritchie
Jennifer B. Gordetsky
Melinda Lerwill
Anna Marie Mulligan

Liron Pantanowitz
David Papke,
Pathologist-in-Training
Carlos Parra-Herran
Rajiv M. Patel
Deepa T. Patil
Charles Matthew Quick
Lynette M. Sholl
Olga K. Weinberg
Maria Westerhoff
Nicholas A. Zoumberos,
Pathologist-in-Training

ABSTRACT REVIEW BOARD

Benjamin Adam
Rouba Ali-Fehmi
Daniela Allende
Ghassan Allo
Isabel Alvarado-Cabrero
Catalina Amador
Tatjana Antic
Roberto Barrios
Rohit Bhargava
Luiz Blanco
Jennifer Boland
Alain Borczuk
Elena Brachtel
Marilyn Bui
Eric Burks
Shelley Caltharp
Wenqing (Wendy) Cao
Barbara Centeno
Joanna Chan
Jennifer Chapman
Yunn-Yi Chen
Hui Chen
Wei Chen
Sarah Chiang
Nicole Cipriani
Beth Clark
Alejandro Contreras
Claudiu Cotta
Jennifer Cotter
Sonika Dahiya
Farbod Darvishian
Jessica Davis
Heather Dawson
Elizabeth Demicco
Katie Dennis
Anand Dighe
Suzanne Dintzis
Michelle Downes

Charles Eberhart
Andrew Evans
Julie Fanburg-Smith
Michael Feely
Dennis Firchau
Gregory Fishbein
Andrew Folpe
Larissa Furtado
Billie Fyfe-Kirschner
Giovanna Giannico
Christopher Giffith
Anthony Gill
Paula Ginter
Tamar Giorgadze
Purva Gopal
Abha Goyal
Rondell Graham
Alejandro Gru
Nilesh Gupta
Mamta Gupta
Gillian Hale
Suntrea Hammer
Malini Harigopal
Douglas Hartman
Kammi Henriksen
John Higgins
Mai Hoang
Aaron Huber
Doina Ivan
Wei Jiang
Vickie Jo
Dan Jones
Kirk Jones
Neerja Kambham
Dipti Karamchandani
Nora Katabi
Darcy Kerr
Francesca Khani

Joseph Khoury
Rebecca King
Veronica Klepeis
Christian Kunder
Steven Lagana
Keith Lai
Michael Lee
Cheng-Han Lee
Madelyn Lew
Faqian Li
Ying Li
Haiyan Liu
Xiuli Liu
Lesley Lomo
Tamara Lotan
Sebastian Lucas
Anthony Magliocco
Kruti Maniar
Brock Martin
Emily Mason
David McClintock
Anne Mills
Richard Mitchell
Neda Moatamed
Sara Monaco
Atis Muehlenbachs
Bitu Naini
Dianna Ng
Tony Ng
Michiya Nishino
Scott Owens
Jacqueline Parai
Avani Pendse
Peter Pytel
Stephen Raab
Stanley Radio
Emad Rakha
Robyn Reed

Michelle Reid
Natasha Rekhman
Jordan Reynolds
Andres Roma
Lisa Rooper
Avi Rosenberg
Esther (Diana) Rossi
Souzan Sanati
Gabriel Sica
Alexa Siddon
Deepika Sirohi
Kalliopi Siziopikou
Maxwell Smith
Adrian Suarez
Sara Szabo
Julie Teruya-Feldstein
Khin Thway
Rashmi Tondon
Jose Torrealba
Gary Tozbikian
Andrew Turk
Evi Vakiani
Christopher VandenBussche
Paul VanderLaan
Hannah Wen
Sara Wobker
Kristy Wolniak
Shaofeng Yan
Huihui Ye
Yunshin Yeh
Anjana Yeldandi
Gloria Young
Lei Zhao
Minghao Zhong
Yaolin Zhou
Hongfa Zhu

To cite abstracts in this publication, please use the following format: **Author A, Author B, Author C, et al. Abstract title (abs#). In "File Title." *Modern Pathology* 2021; 34 (suppl 2): page#**

33 YAP1 Immunohistochemistry in Epithelioid Hemangioendothelioma Variant with YAP1-TFE3 Fusion

William Anderson¹, Christopher Fletcher², Jason Hornick¹

¹Brigham and Women's Hospital, Harvard Medical School, Boston, MA, ²Brigham and Women's Hospital, Boston, MA

Disclosures: William Anderson: None; Christopher Fletcher: None; Jason Hornick: None

Background: Epithelioid hemangioendothelioma (EHE) with *YAP1-TFE3* fusion is a recently characterized distinctive variant of EHE that accounts for a small subset (<5%) of cases. This tumor type is composed of nests of epithelioid cells with voluminous pale cytoplasm and often shows focally vasoformative architecture. TFE3 immunohistochemistry (IHC) can be used to support the diagnosis; however, studies have questioned its specificity. Yes-associated protein 1 (YAP1), part of the Hippo signaling pathway, is expressed in normal endothelial cells, but becomes disrupted in EHE variant with *YAP1-TFE3*, such that only a small N-terminal region of YAP1 is expressed in the fusion protein. We hypothesized that IHC using an antibody directed against the C-terminus of YAP1 would be negative in this tumor type. The purpose of this study was to evaluate YAP1 C-terminus IHC in EHE with *YAP1-TFE3* and other epithelioid vascular neoplasms in the differential diagnosis.

Design: In total, 72 tumors were included in this study, encompassing 5 tumor types: EHE with *YAP1-TFE3* (n=12), conventional (CAMTA1-positive) EHE (n=20), pseudomyogenic hemangioendothelioma (n=10), epithelioid hemangioma (n=20) and epithelioid angiosarcoma (n=10). IHC was performed using a rabbit monoclonal anti-YAP1 C-terminus antibody. CAMTA1, TFE3, and FOSB IHC was performed in selected cases.

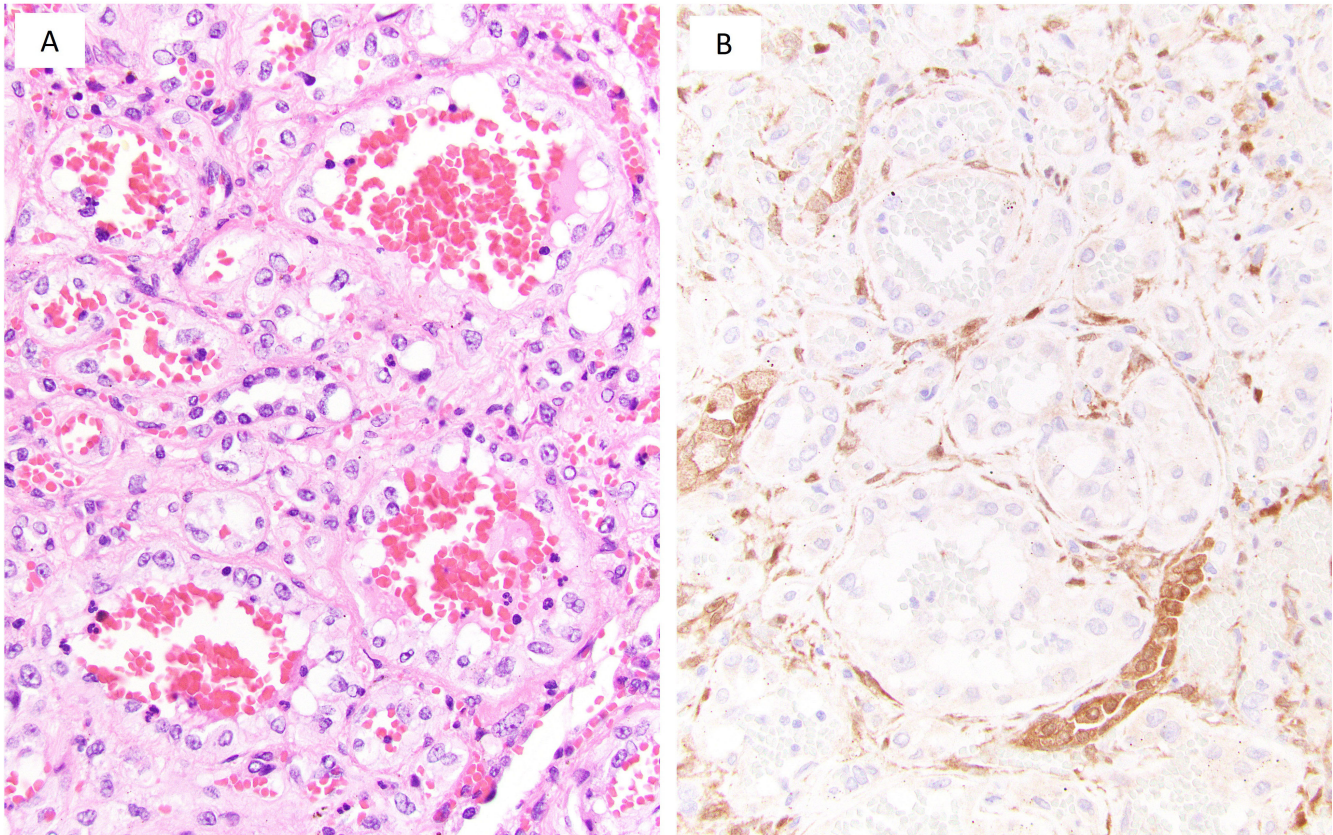
Results: Results of YAP1 IHC are summarized in Table 1. EHE with *YAP1-TFE3* showed complete loss of YAP1 C-terminus expression in 9 of 12 (75%) cases (Figure 1). Three cases showed retained YAP1 expression, 2 with weak cytoplasmic staining and 1 with strong nuclear and cytoplasmic staining. Loss of YAP1 was seen in one conventional EHE (1/20; 5%). Among other epithelioid vascular tumors, only one case showed loss of YAP1. IHC for TFE3 was positive in all cases of EHE with *YAP1-TFE3*. Weak staining was observed in one conventional EHE. CAMTA1 was negative in all EHE with *YAP1-TFE3* tested (0/7).

Table 1. YAP1 C-terminus immunohistochemistry in epithelioid vascular neoplasms.

Tumor type	Total cases	YAP1 loss (%)	YAP1 retention (%)
Epithelioid hemangioendothelioma with <i>YAP1-TFE3</i>	12	9 (75)	3 (25)
Epithelioid hemangioendothelioma with <i>WWTR1-CAMTA1</i>	20	1 (5)	19 (95)
Pseudomyogenic hemangioendothelioma	10	0 (0)	10 (100)
Epithelioid hemangioma	20	1 (5)	19 (95)
Epithelioid angiosarcoma	10	0 (0)	10 (100)

Figure 1 - 33

Figure 1. A. Epithelioid hemangioendothelioma with *YAP1-TFE3* fusion shows well-formed blood vessels lined by epithelioid cells with abundant eosinophilic cytoplasm. B. Immunohistochemistry for YAP1 C-terminus shows loss of expression. In this case entrapped lung parenchyma serves as a positive control.



Conclusions: EHE with *YAP1-TFE3* usually shows loss of YAP1 C-terminus expression. YAP1 IHC is highly specific (97%) for this EHE variant, as loss of staining was only observed in 2/60 other epithelioid vascular neoplasms. YAP1 C-terminus IHC is a useful marker that supports the diagnosis of EHE with *YAP1-TFE3*. This marker should be used in a panel with TFE3 and CAMTA1.

34 Nuclear Expression of DDIT3 Distinguishes High-Grade Myxoid Liposarcoma from other Round Cell Sarcomas

Esther Baranov¹, Margaret Black², Christopher Fletcher¹, Gregory Charville³, Jason Hornick⁴
¹Brigham and Women's Hospital, Boston, MA, ²Stanford Health Care, Palo Alto, CA, ³Stanford Medicine/Stanford University, Stanford, CA, ⁴Brigham and Women's Hospital, Harvard Medical School, Boston, MA

Disclosures: Esther Baranov: None; Margaret Black: None; Christopher Fletcher: None; Gregory Charville: None; Jason Hornick: None

Background: Myxoid liposarcoma (MLPS), a malignant adipocytic neoplasm with a predilection for the extremities, comprises up to 30% of liposarcomas overall. MLPS is genetically defined by a recurrent t(12;16) translocation leading to the FUS-DDIT3 fusion oncoprotein (90% of cases) or more rarely t(12;22) leading to EWSR1-DDIT3. Low-grade MLPS is characterized by bland spindle cells within a myxoid matrix containing delicate “chicken-wire” vasculature, while high-grade (“round cell”) MLPS often mimics other round cell sarcomas. In many

cases, cytogenetic or molecular genetic techniques are applied to confirm the diagnosis. A recent study has documented the utility of DDIT3 immunohistochemistry (IHC) using a novel monoclonal antibody in the differential diagnosis of myxoid soft tissue tumors. The purpose of this study was to evaluate DDIT3 IHC as a surrogate for molecular testing in high-grade MLPS.

Design: Immunohistochemistry (IHC) was performed using a mouse monoclonal antibody directed against the N-terminus of DDIT3 (clone 9C8; Abcam). IHC was performed on whole tissue sections from 50 high-grade MLPS cases (27 genetically confirmed; 11 with pure round cell morphology) and 317 histologic mimics used as controls (168 on whole sections and 149 on a tissue microarray). Histologic mimics included Ewing sarcoma; *CIC*-rearranged sarcoma; sarcomas with *BCOR* genetic alterations; poorly differentiated synovial sarcoma; alveolar and embryonal rhabdomyosarcomas; mesenchymal chondrosarcoma; desmoplastic small round cell tumor; and neuroblastoma. Nuclear staining in >5% of cells was considered positive.

Results: By IHC, 47 (94%) high-grade MLPS showed strong diffuse nuclear staining for DDIT3 (>95% of cells). Of the three remaining cases, one showed 4+ staining, one showed weak 1+ staining and one was entirely negative (Table 1). These cases, all with genetically confirmed *DDIT3* rearrangement, were among the oldest in the study (from 2015). Of the controls, 2% of cases were positive, most notably Ewing sarcoma, with no more than 25% nuclear staining. An additional 19% of controls displayed less than 5% nuclear staining manifesting as scattered rare cells or clusters of cells around areas of necrosis. Overall, DDIT3 IHC showed 96% sensitivity and 98% specificity for MLPS.

TABLE 1. Summary of Immunohistochemical Staining for DDIT3

Tumor type	Total Cases	Positive (%) ¹	0	1+	2+	3+	4+	5+
Myxoid liposarcoma, high grade	50	48 (96)	1	1	0	0	1	47
Pure "round cell" morphology	11	11 (100)	0	0	0	0	0	11
Histologic mimics	317	6 (2)	251	60	6	0	0	0
Alveolar rhabdomyosarcoma	36	0 (0)	32	4	0	0	0	0
Sarcomas with <i>BCOR</i> genetic alterations	20	1 (5)	12	7	1	0	0	0
<i>CIC</i> -rearranged sarcoma	20	0 (0)	10	10	0	0	0	0
Desmoplastic small round cell tumor	37	1 (3)	29	7	1	0	0	0
Embryonal rhabdomyosarcoma	74	1 (1)	65	8	1	0	0	0
Ewing sarcoma	38	3 (8)	24	11	3	0	0	0
Mesenchymal chondrosarcoma	20	0 (0)	14	6	0	0	0	0
Neuroblastoma	47	0 (0)	47	0	0	0	0	0
Synovial sarcoma, poorly differentiated	25	0 (0)	18	7	0	0	0	0

0 (0%); 1+ (<5%); 2+ (5-25%); 3+ (26-50%); 4+ (51-75%); 5+ (76-100%)

¹Positivity was defined as the presence of nuclear staining in greater than 5% of cells.

Figure 1 - 34

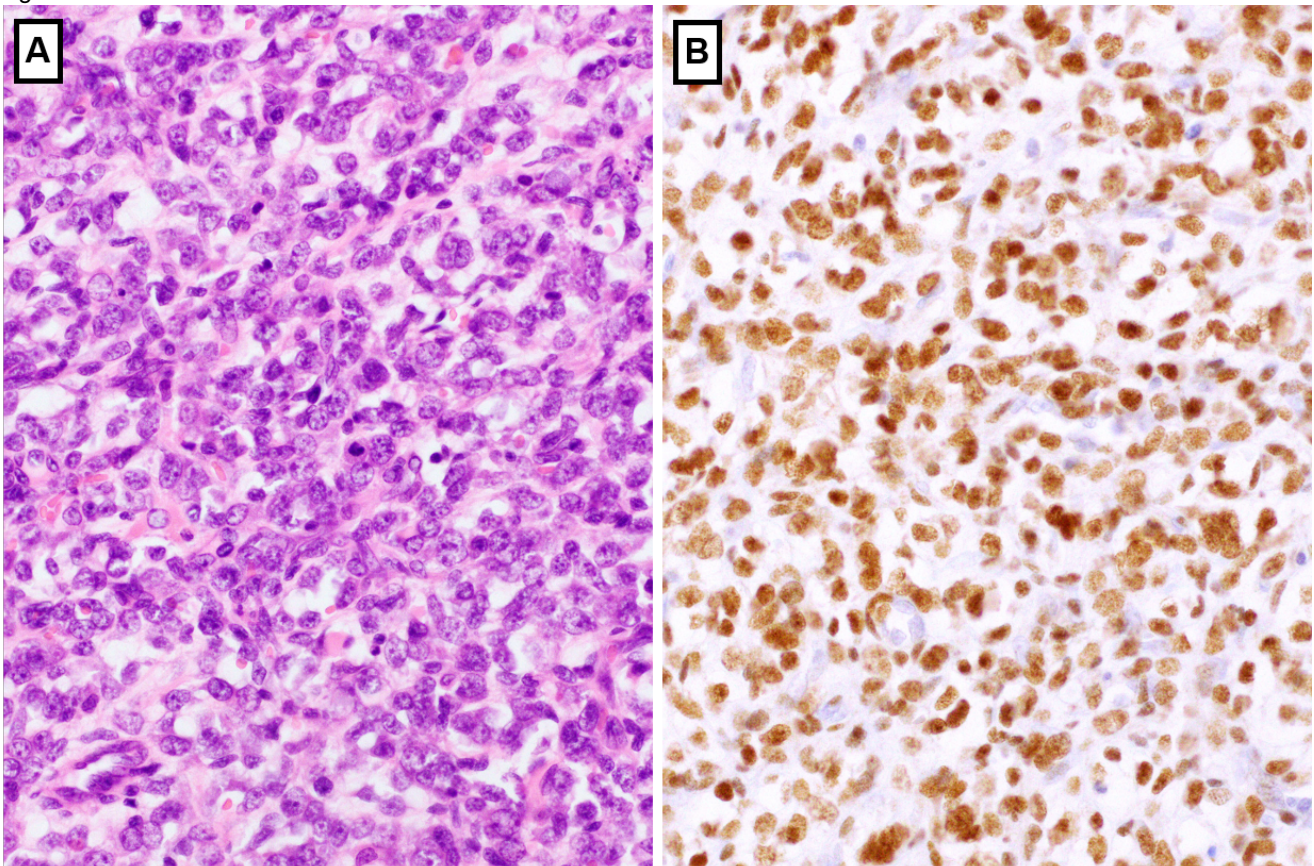


Figure 1. High-grade myxoid liposarcoma with pure round cell morphology (A). Immunohistochemistry for DDIT3 shows strong diffuse nuclear positivity (B).

Conclusions: IHC using an antibody directed against the N-terminus of DDIT3 is highly sensitive and specific for high-grade MLPS among histologic mimics. IHC using this antibody could replace molecular genetic testing in most cases.

35 Fibrous Dysplasia Protuberans: A Rare Entity

Mohadese Behtaj¹, Muhammad Hakim¹, Jaylou Velez Torres¹, G. Pétur Nielsen², Elizabeth Montgomery¹, Andrew Rosenberg³

¹University of Miami Miller School of Medicine, Miami, FL, ²Massachusetts General Hospital, Harvard Medical School, Boston, MA, ³University of Miami Health System, Miami, FL

Disclosures: Mohadese Behtaj: None; Muhammad Hakim: None; Jaylou Velez Torres: None; G. Pétur Nielsen: None; Elizabeth Montgomery: None; Andrew Rosenberg: None

Background: Fibrous dysplasia (FD) is the most common fibro-osseous bone tumor, accounting for 7% of primary bone tumors, and results from somatic activating mutation of GNAS gene. In the skeleton, it is monostotic or polyostotic, and solitary lesions account for 70-80% of cases. FD originates in the medullary canal, is well-circumscribed, and is usually confined to the bone but may be expansile. The expanded exophytic variant of FD distorts the bone and causes severe deformity, and can be confused clinically with aggressive neoplasms. This variant of FD, also known as FD protuberans (FDP) is extremely uncommon. To increase our understanding of this tumor we report our experience with 9 cases.

Design: The cases were identified retrospectively from the surgical pathology files of the contributing institutions and the consultation files of one of the authors.

Results: The 9 cases included 6 males and 3 females, who ranged in age from 13-69 years (mean 42.4). 5 patients had polyostotic disease, and 1 patient had McCune-Albright syndrome. 6 cases involved the rib, 2 developed in the craniofacial bones, and one case involved the iliac crest. The largest dimension of the tumor ranged from 7.5-28 cm. Radiologically the tumors were large, massively expansile in an eccentric fashion, had well-defined sclerotic margins and ground glass radiodensity (Figure 1 and 2). Microscopically they were composed of benign spindle cells arranged in a storiform pattern associated with curvilinear trabeculae of woven bone that lacked conspicuous osteoblastic rimming. They lacked a permeative growth pattern, significant cytological atypia, mitotic activity, and soft tissue invasion and were always confined by periosteum. One patient with a large facial mass expired from complication of surgical removal, and 2 cases with follow-up showed no evidence of disease 3 and 8 years after resection. None of our cases had sarcomatous transformation.

Figure 1 - 35



Figure 1. Reformatted 3D sagittal CT image of fibrous dysplasia protuberans involving face. The tumor is large, massively expansile and eccentric.

Figure 2 - 35



Figure 2. Sagittal view of CT scan of fibrous dysplasia protuberans, polyostotic, involving left second and fourth ribs. The tumor bulges into the lung.

Conclusions: FDP is rare and presents as a large, eccentric mass that can be severely deforming and clinically concerning for a variety of types of neoplasms. It often occurs in the setting of polyostotic disease, and 10% of patients have McCune-Albright syndrome. Pathologists should be aware of this unusual variant of FD, so it is not confused with other types of neoplasms in the differential diagnosis.

36 PDL1 Expression in Sarcomas

Marilyn Bui¹, Evita Henderson-Jackson¹, Farah Khalil¹, Andrew Brohl¹, Joseph Johnson¹, Tingan Chen¹
¹H. Lee Moffitt Cancer Center & Research Institute, Tampa, FL

Disclosures: Marilyn Bui: None; Evita Henderson-Jackson: None; Farah Khalil: None; Andrew Brohl: *Advisory Board Member, Bayer; Advisory Board Member, EMD Serono; Advisory Board Member, Deciphera*; Joseph Johnson: None; Tingan Chen: None

Background: Immunotherapy targeted to PD1/PDL1 is an emerging potential treatment for select sarcomas. Early investigations of anti-PD1 therapy in sarcoma suggest that tumor PDL1 expression may help to predict response to checkpoint inhibition. Given the rarity and heterogeneity of sarcoma, the incidence of PDL1 expression across

sarcoma types is incompletely defined. The aim of this study was to evaluate PDL1 expression in a cohort sarcoma cases and their relationship with prognosis.

Design: Sarcoma histology sections and tissue microarray (TMA) of osteosarcoma, leiomyosarcoma, and Ewing sarcoma were subjected to PDL1 22C3 KETYUDA (FDA) GP immunohistochemical (IHC) study. TMA slides were scanned with an Aperio™ ScanScope AT2 (Leica Biosystems, Vista, CA) with a 200x/0.8NA objective lens. Using the eSlide Manager database and the TMA module, the images were segmented and scored by the Positive Pixel Count (PPC) v9 algorithm. The % positivity was scored using these automated methods for the TMAs and for clinical samples was manually verified and a combined positive score (CPS) calculated by sarcoma pathologist certified in PDL1 interpretation.

Results: Utilizing a cut-off of $\geq 1\%$ staining, in the TMAs PDL1 was positive in 24.8% (40/161 cores) of osteosarcoma, 44.7% (17/38 cores) of Ewing sarcoma, and 36.6% (49/134 cores) of leiomyosarcoma. PDL1 was positive (CPS $\geq 1\%$) in 53.3% (16/30) of clinically tested sarcomas, which included a variety of sarcoma subtypes. Correlation analysis with clinical features such as tumor grade, stage and survival is ongoing and will be presented.

Conclusions: This study shows that PDL1 is expressed in a clinically meaningful percentage of a variety of sarcoma subtypes. A high rate of PDL1 positivity in clinically tested samples likely reflects in part a selection bias towards testing of potentially immunoresponsive sarcoma subtypes. Additional study is underway to verify automated PDL1 staining quantification and to perform correlation analysis of PDL1 status with clinical outcomes.

37 Clinicopathologic and Molecular Features of Denosumab-Treated Giant Cell Tumor of Bone: Analysis of 21 Cases

Hong Cheng¹, Li Yang², Hongjuan Zhang², Yingmei Wang²

¹The Fifth Affiliated Hospital of Zhengzhou University, Zhengzhou, China, ²Xijing Hospital, the Air Force Medical University, Xi'an, China

Disclosures: Hong Cheng: None; Li Yang: None; Hongjuan Zhang: None; Yingmei Wang: None

Background: Denosumab, a monoclonal antibody of Receptor Activator of Nuclear factor Kappa-B Ligand (RANKL), is used as a treatment for selected cases of giant cell tumor of bone (GCTB) that are unresectable or where surgical resection would likely result in excessive morbidity. It has been reported that GCTB exhibits diverse morphological changes after denosumab treatment, posing diagnostic challenges. We summarized clinicopathologic and molecular features of 21 cases of denosumab-treated GCTB (DT-GCTB).

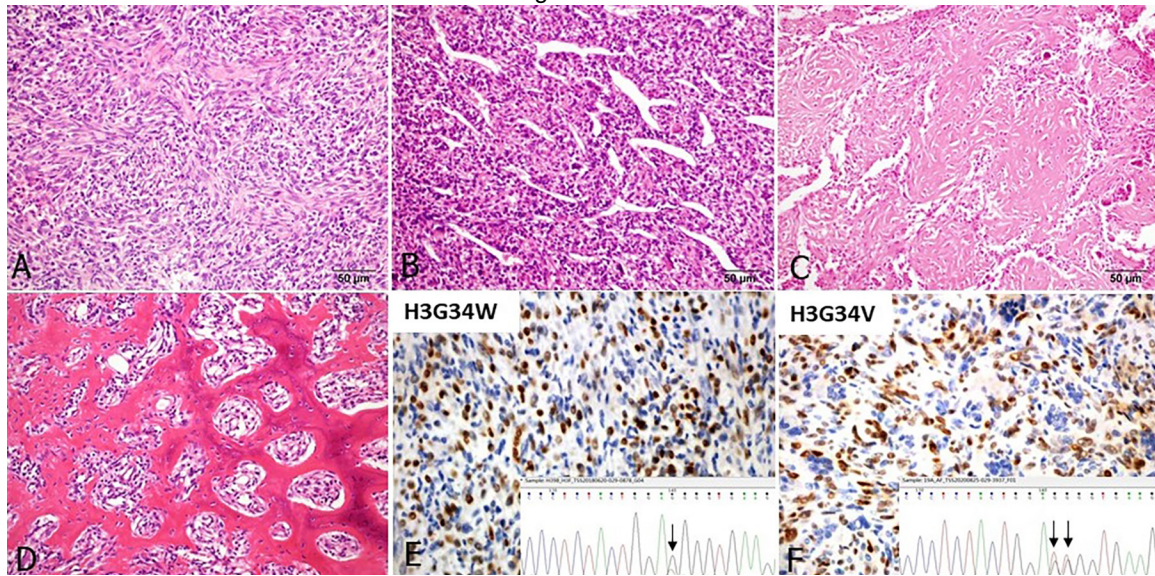
Design: Twenty one biopsy-confirmed, post-denosumab-therapy GCTB cases were collected from institutional archives. Clinicopathological data were analyzed. Somatic mutation on glycine 34 of histone H3 was studied using immunohistochemical (IHC) stain for H3G34W, H3G34V and H3G34R. Histone H3 encoding gene H3F3A mutation status was verified by direct Sanger sequencing.

Results: The cohort included 21 cases (13 females, 8 males) with DT-GCTB. Radiographically, there were development of sclerotic neocortex and varying degrees of matrix osteosclerosis. Histopathological features included a marked depletion of osteoclast-like giant cells, different degree of ossification, fibrosis, and proliferation of mononuclear cells. In addition, 7 cases (33.3%) showed complete elimination of osteoclast-like giant cells; 1 case (4.8%) had focal residual classic GCTB, and 2 cases (9.5%) manifested mild nuclear atypia. These morphological variations could mimic other lesions such as fibrous dysplasia, juvenile ossifying fibroma, non-ossifying fibroma, osteblastoma, sclerosing epithelioid fibrosarcoma and conventional osteosarcoma. We further performed IHC staining for H3G34W, which was positive in 19 cases (90.5%). As one of the important features in post-therapy tumors, there were still abundant H3G34W positive cells in these cases. The two H3G34W negative cases were further stained with H3G34V and H3G34R antibodies, one of which was positive for H3G34V. The H3F3A mutation status was verified by direct Sanger sequencing. G34W mutation was confirmed in 16 of 16 successfully tested cases (100%). The G34V positive staining was actually due to cross reaction to histone with G34L mutation.

Figure 1 - 37



Figure 2 - 37



Conclusions: DT-GCTB can show a spectrum of morphology including a striking giant cells depletion and massive intralesional bone deposition. While the tumors can differ significantly from the conventional GCTB morphologically, they still exhibit similar histone H3 mutation profile. Clinical history of denosumab administration, radiographic findings, awareness of the histological features of DT-GCTB, and IHC and molecular studies for histone H3 mutations are important to avoid misdiagnosis.

38 mGluR1 is a Sensitive and Specific Immunohistochemical Marker for Chondromyxoid Fibroma

Jonathan Davick¹, Alexandra Isaacson², Andrew Bellizzi²

¹University of Iowa Carver College of Medicine, IA, ²University of Iowa Hospitals & Clinics, Iowa City, IA

Disclosures: Jonathan Davick: None; Alexandra Isaacson: None; Andrew Bellizzi: None

Background: Chondromyxoid fibroma (CMF) is a rare cartilaginous bone tumor with morphologic features overlapping with other chondroid and myxoid bone tumors. Prognosis is excellent with curettage or conservative en bloc resection. Given CMF’s rarity and occasional cytologically atypical “pseudomalignant” cases, the diagnosis may be challenging. CMF was recently shown to be driven by *GRM1* gene fusion and promoter swapping (most often with *COL12A1*) leading to marked overexpression of metabotropic glutamate receptor 1 (mGluR1; the protein encoded by *GRM1*). We hypothesized that mGluR1 immunohistochemistry (IHC) would be useful in the distinction of CMF from diagnostic mimics.

Design: We optimized a mGluR1 rabbit monoclonal antibody (clone JM11-61) for IHC, which was subsequently performed on our institutional cohort of CMFs (n=24) and a series of 70 potential diagnostic mimics, including chondroblastoma (n = 20), giant cell tumor of bone (n = 13), grade 1 chondrosarcoma (n = 8), grade 2 chondrosarcoma (n = 9), high-grade and dedifferentiated chondrosarcoma (n = 3), chondroblastic osteosarcoma (n = 7), enchondroma (n = 9), and myxoma of bone (n = 1). Intensity (0-3+) and extent (0-100%) of mGluR1 staining was evaluated. Sensitivity and specificity was calculated at two positivity thresholds: 1.) low threshold—defined as any definite immunoreactivity (i.e., ≥1+ in ≥1% of tumor cells) and 2.) high threshold—defined as strong, readily identifiable positivity (i.e., ≥2+ in ≥20% of tumor cells).

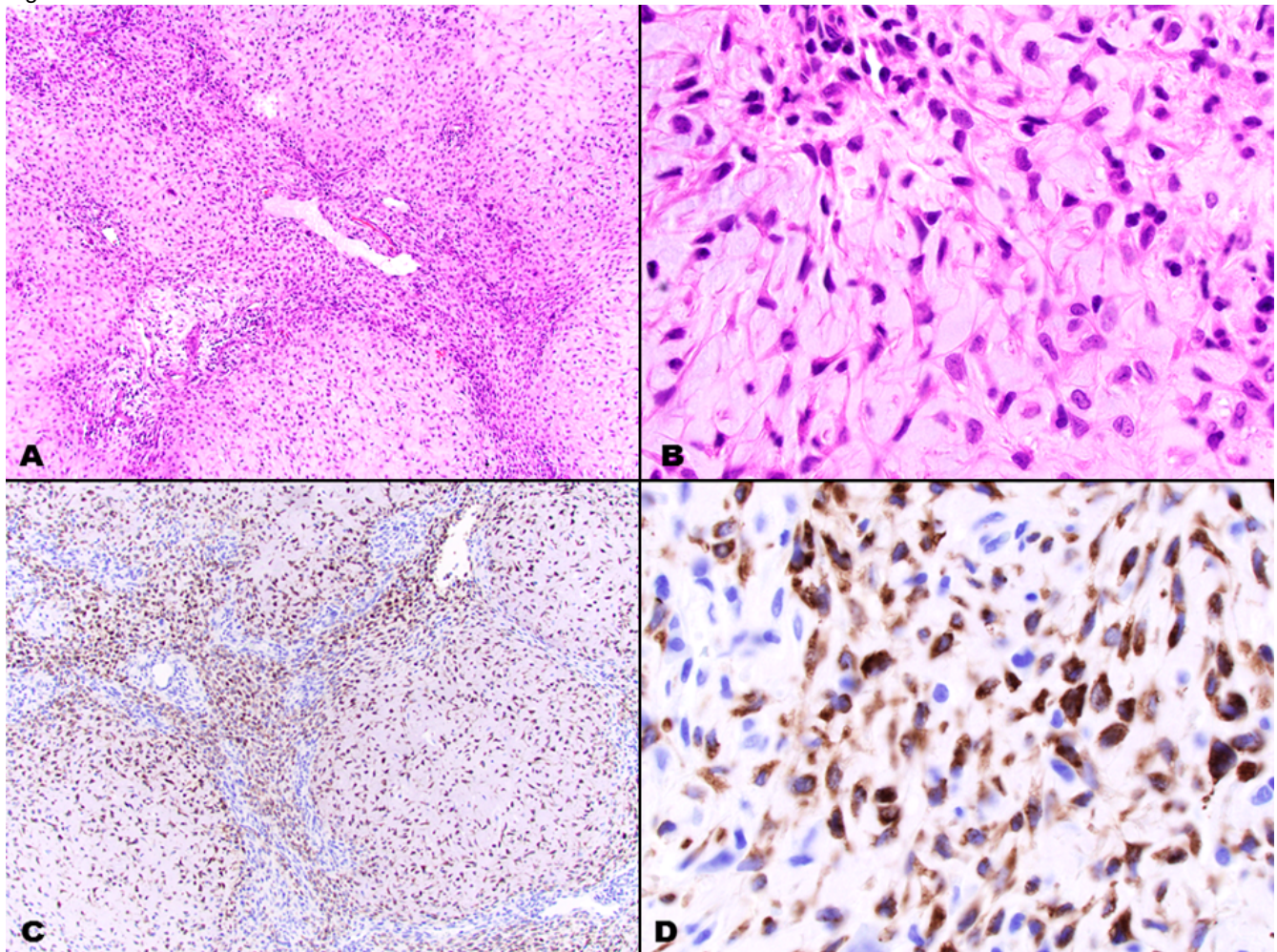
Results: Results are summarized in table 1 and illustrated in figure 1. 88% of CMFs were mGluR1-positive at the low threshold, while only 1 non-CMF (grade 2 chondrosarcoma) was (low threshold sensitivity = 88%, specificity = 99%). Using the high threshold, 71% of CMFs and none of the non-CMFs were positive (high threshold sensitivity = 71%, specificity = 100%).

Table 1:

	Low positive threshold			High positive threshold	
	CMF	Non-CMF		CMF	Non-CMF
mGluR1 positive	21	1	mGluR1 positive	17	0
mGluR1 negative	3	69	mGluR1 negative	7	70
	88%	99%		71%	100%
	sensitivity	specificity		sensitivity	Specificity

Figure 1 caption: Hematoxylin and eosin-stained section of a chondromyxoid fibroma at 100x (A) and 500x magnification (B). mGluR1 IHC performed on the same case at 100x (C) and 500x magnification (D).

Figure 1 - 38



Conclusions: mGluR1 is a novel sensitive and specific immunohistochemical marker for CMF, which could aid the pathologist in distinguishing CMF from diagnostic mimics.

39 Novel Synthetic Lethality (SL) anti-Cancer Drug Target in Sarcomas Based on MTAP Genomic Loss (MTAP loss)

Brennan Decker¹, Talal Ahmad², Douglas Mata¹, Tyler Janovitz¹, J. Keith Killian¹, Richard Huang³, Douglas Lin¹, Shakti Ramkissoon⁴, Ole Gjoerup¹, Natalie Danziger¹, Jeffrey Ross⁵

¹Foundation Medicine, Inc., Cambridge, MA, ²Upstate Medical University, New York, NY, ³Foundation Medicine, Inc., Cary, NC, ⁴Foundation Medicine, Inc., Morrisville, NC, ⁵Upstate Medical University, Syracuse, NY

Disclosures: Brennan Decker: *Employee*, Foundation Medicine; Talal Ahmad: *None*; Douglas Mata: *Employee*, Foundation Medicine, Inc.; Tyler Janovitz: *Employee*, Foundation Medicine; J. Keith Killian: *Employee*, Foundation Medicine; Richard Huang: *Speaker*, Foundation medicine; Douglas Lin: *Employee*, Foundation Medicine, Inc.; *Stock Ownership*, Roche; Shakti Ramkissoon: *Employee*, Foundation Medicine; Ole Gjoerup: *None*; Natalie Danziger: *Employee*, Foundation Medicine Inc.; Jeffrey Ross: *Employee*, Foundation Medicine; *Advisory Board Member*, Tango Therapeutics

Background: Sarcomas arising in soft tissues and visceral organs are frequently aggressive malignancies with limited therapy options when metastatic disease develops. Among treatment strategies that have recently emerged, the finding of new SL targets such as PRMT5 exploiting the genomic loss of *MTAP* have received considerable attention.

Design: 140,182 cases of clinically advanced and metastatic cancer underwent hybrid-capture based comprehensive genomic profiling using the F1CDx FDA-approved assay to evaluate all classes of genomic alterations (GA). Tumor mutational burden (TMB) was determined on 0.8 Mbp of sequenced DNA and microsatellite instability (MSI) was determined on 95 loci. PD-L1 expression was determined by IHC (Dako 22C3).

Results: 12,617 (9.0%) total cases pan-cancer featured *MTAP* loss. In subset of 1,230 sarcomas, 128 (10.4%) featured *MTAP* loss with GISTs having a 40% *MTAP* loss and non-GIST sarcomas 5.0%. *MTAP* loss was found in MPNST (20%), bone sarcomas (4-12%), cardiopulmonary/vascular sarcomas (2-7%), soft tissue sarcomas (0-4%) and uterine sarcomas (1-3%). *MTAP* loss sarcomas feature a higher GA/tumor than *MTAP* intact tumors but this difference is not significant when the *MTAP/CDKN2A/B* delicon on chromosome 9 is excluded from the analysis. GA in *KIT* are significantly higher in *MTAP* loss tumors (P=.01) reflecting the high proportion of GISTs in the *MTAP* loss group. In the *MTAP* loss MPNST, all (100%) cases featured the homozygous chromosome 9 delicon and germline truncating *NF1* GA. GA in *TP53* are lower in *MTAP* Loss sarcomas (P=.03). *ARID1A* mutations were more frequent in the *MTAP* loss sarcomas. (P=.01). Examining biomarkers of potential immuno-oncology (IO) drug response, including MSI and PD-L1 expression were not significantly different but median TMB was higher (p=.01) in the *MTAP* loss vs *MTAP* intact sarcomas.

	Sarcoma <i>MTAP</i> Intact	Sarcoma <i>MTAP</i> Loss	Significance
Number of Cases	1,102	128	
Males/Females	50%/50%	53%/47%	NS
Median age (range) years	61 (1-89+)	65 (7-89+)	NS
GA/tumor	2.8	5.5	NS*
Gene Rearrangements	16%	15%	NS
<i>CDKN2A</i>	15%	100%	P<.0001
<i>CDKN2B</i>	9%	90%	P<.0001
<i>TP53</i>	23%	14%	P=.03
<i>TERT</i>	5%	4%	NS
<i>KIT</i>	40%	52%	P=.01
<i>PIK3CA</i>	4%	6%	NS
<i>ARID1A</i>	2%	6%	P=.01
<i>NF1</i>	7%	6%	NS
<i>NF2</i>	1%	3%	NS
<i>PTEN</i>	4%	6%	NS
MSI High	0%	0%	NS
Median TMB	1.3	2.5	P=.01
TMB>10 mut/Mb	3%	2%	NS
TMB>20 mut/Mb	2%	1%	NS
PD-L1 Low Positive	9%	21%	NS
PD-L1 High Positive	8%	3%	NS

Conclusions: *MTAP* deletion occurs in more than 10% of sarcomas in a wide variety of histologic subtypes, including GIST and non-GIST tumors. With the exception of *KIT*-directed therapy in GIST, both *MTAP* intact and *MTAP* deleted sarcomas feature relatively limited targeted therapy and immunotherapy opportunities. Further study of anti-PRMT5 drugs that are enabled by *MTAP* loss in sarcomas appears warranted.

40 Primary Superficial Extraskelatal Osteosarcoma: Clinicopathologic Features of 4 Cases

Carina Dehner¹, Justin Hicks², Cara Cipriano¹, John Chrisinger¹

¹Washington University School of Medicine, St. Louis, MO, ²Washington University School of Medicine in St. Louis, St. Louis, MO

Disclosures: Carina Dehner: None; Justin Hicks: None; Cara Cipriano: None; John Chrisinger: None

Background: Extraskelatal osteosarcoma (ESOS) is an uncommon osteogenic tumor that usually pursues a highly aggressive clinical course. While the large majority of ESOS arise in the deep soft tissues, superficial cases are rarely encountered and require special clinical and differential diagnostic considerations. We describe the clinicopathologic features of four cases of primary superficial ESOS.

Design: A retrospective archival search was performed for primary superficial ESOS. Slides were reviewed for diagnosis verification and confirmation of superficial site (tumor entirely superficial to the superficial fascia). Available radiographic imaging studies were also reviewed to confirm the absence of deeper tumor. Demographic, preoperative clinical impressions, prior history of cancer, tumor site, tumor size, procedure type, resection margin status, neoadjuvant/adjuvant treatment, local recurrence, metastasis, follow-up time and status at last follow-up were also noted.

Results: Four cases of primary superficial ESOS were identified. Patients (all male) ranged in age from 33-72 years old (median 57.5). All tumors presented on the extremities: thigh (2), calf (1) and elbow (1) and initial clinical findings suggested a broad differential diagnosis including epidermal inclusion cyst (1), ganglion/synovial cyst (1) and nodular melanoma vs pyogenic granuloma vs infection (1). In the fourth case, the clinical impression was not clear but the tumor was noted to have been present for 2-3 years. Cancer histories included lung adenocarcinoma (1) and Hodgkin lymphoma (1). None of the tumors arose in a radiation field. All tumors were excised/re-excised to negative margins. Tumors ranged in size from 2.1-6.0 cm (median 2.7). In all cases, histologic examination showed highly cellular pleomorphic and spindle cell neoplasms with osteoid deposition. Evidence of epithelial or melanocytic differentiation was not identified. Whole body imaging studies did not demonstrate an underlying occult primary site. The median follow-up time was 22 months (range: 5.5-36) and none of the 4 patients experienced local recurrence or distant metastasis.

Conclusions: Primary superficial ESOS is an extremely rare neoplasm that frequently clinically mimics a benign process. Careful microscopic examination, and correlation with clinical history of imaging findings is important to exclude metastasis from a deep-seated primary osteosarcoma and heterologous osteosarcomatous differentiation in other neoplasms. Larger long-term studies are needed for confirmation, however in our small study the prognosis of primary superficial ESOS appears more favorable likely due to smaller tumor size and surgical accessibility.

41 Dedifferentiated Chondrosarcoma with Minimal Dedifferentiated Component

Carina Dehner¹, Nolan Maloney², Wei-Lien (Billy) Wang², Douglas McDonald¹, John Chrisinger¹

¹Washington University School of Medicine, St. Louis, MO, ²The University of Texas MD Anderson Cancer Center, Houston, TX

Disclosures: Carina Dehner: None; Nolan Maloney: None; Wei-Lien (Billy) Wang: None; Douglas McDonald: None; John Chrisinger: None

Background: Dedifferentiated chondrosarcoma (DDCS) is a rare and highly aggressive bone sarcoma which is characterized by a low to intermediate grade hyaline cartilage component with an abrupt transition to a high-grade non-chondrosarcomatous component, most frequently undifferentiated sarcomatous or osteosarcomatous. While more favorable prognostic factors include non-pelvic location, margin negative resection, absence of pathologic fracture, size <8 cm and dedifferentiation <50%, the overall prognosis is bleak. In majority of cases, the dedifferentiated component is large. However, rarely cases can only have minimal or small areas of dedifferentiation. We evaluated the prognostic significance of this finding compared to DDCS with large dedifferentiation.

Design: The departmental pathology archives of two institutions were retrospectively searched. At institution 1, all primary resections for DDCS were pulled, while at institution 2 all primary resections with "minimal" or "early" DDCS were retrieved. Available slides were reviewed for diagnosis confirmation, resection margin status, extraosseous extension, size of dedifferentiated (DD) component, DD component focality, mitotic rate and tumor necrosis. Site, tumor size, imaging impression, local recurrence, distant metastases, overall survival and follow-up duration were also noted.

Results: Thirty cases met criteria and were included. Patients (18 male, 12 female) ranged in age from 37-79 years (mean 61). Tumors involved the femur (15), innominate (5), sacrum (1), tibia (3), fibula (1), humerus (2), sternum (2) and rib (1). Mean tumor size was 14 cm (range 3.6-37). The DD component size ranged from 0.1 to 37 cm and was unifocal (22), multifocal (4) and focality unknown (4). The mean follow-up time was 37 months (range 2-163). Ten tumors recurred locally and 15 developed distant metastases. In three patients the DD component was <1 cm and two were alive with no evidence of disease (ANED) at 13 and 65 months, while the third patient died of

metastatic sarcoma at 48 months. In an additional three cases, the DD component was between 1-2 cm, and 2 of these patients were ANED at 129 and 163 months, while the third died of metastatic sarcoma at 8 months.

Conclusions: DDCS are high-grade sarcomas which frequently recur and metastasize. In our limited sample, it appears that DDCS with DD component <1 cm and perhaps even <2 cm may show a more variable outcome. However, it should be noted that even small foci of DD can have an aggressive course highlighting the need of careful gross and microscopic examination.

42 Spinal (Cord) Lipoma is Morphologically Identical to Lipomatosis of (Median) Nerve and Similarly Demonstrates pAKT (PIK3CA) Upregulation

Julie C. Fanburg-Smith¹, Charles S. Specht¹, Mark S. Dias¹

¹Penn State Health Milton S. Hershey Medical Center, Hershey, PA

Disclosures: Julie C. Fanburg-Smith: None; Charles S. Specht: None; Mark S. Dias: None

Background: Lipomatosis of nerve (fibrolipomatous hamartoma of median nerve) occurs due to overgrowth of fibroadipose tissue within epineurium and is associated with macrodactyly and *PIK3CA* upregulation. Spinal lipoma, including lipomyelomeningocele and fatty filum terminale, is considered an occult congenital dysraphism formed by aberrant primary or secondary tube neurulation. This can lead to adipocytic overgrowth and non-functional nerve tethering of the spinal cord to overlying soft tissue and skin. After an index case of spinal lipoma resembled features of lipomatosis of (median) nerve, we wanted to understand the clinicopathologic and genetic features of our cases of spinal cord lipoma.

Design: Cases coded as “spinal lipoma” were collected from our pathology and clinical files. Clinicopathologic data and glass slides were reviewed and immunostained with PTEN and pAKT (*PIK3CA* upregulation). Classic lipomatosis of median nerve with macrodactyly was used for comparison control.

Results: 32 spinal lipomas included 55% female and 45% male, with a bimodal age distribution: 69% children (50% less than 1 year, range 2 months to 14 years) and 31% adults (median age 38 years, range 26-57), ages overall ranged 2 months to 57 years. Patients were clinically referred because of other malformation sequences (anorectal malformation or caudal duplication), a visible cutaneous hemangioma, dimple or fatty mass in the lumbar spine, and/or sensorimotor, urological, or orthopedic deterioration. Associated syndromes included VACTERL, Trisomy 21, Duane, and Klippel Feil. MRI disclosed typical fatty masses that infiltrated the underlying tethered spinal cord or filum terminale. Some cases involved both spinal cord and subcutaneous adipose tissue. Surgical treatment of spinal lipoma successfully detached the spinal cord from the adipose tissue and freed or untethered the spinal cord, preventing further neuronal damage. Microscopically, all cases revealed a medium-sized hypertrophic nerve with perineural fibrous thickening, separated small nerve branches with neuroma-like onion-skinning fibrosis pattern and stranded fibrous tissue throughout abundant mature adipose tissue. Vessels and occasional smooth or skeletal muscle were observed. All spinal lipomas and median nerve lipomatosis control upregulated pAKT (MTOR pathway, *PIK3CA*), specifically localized to fat and nerve, without evidence for PTEN mutation.

Conclusions: This is a novel previously-unreported observation that spinal lipoma with dysraphism has identical morphology and pAKT (*PIK3CA*, MTOR pathway) upregulation as lipomatosis of median nerve with macrodactyly. Surgical untethering reduces stretch injury of the spinal cord and prevents further neurologic compromise. Recognizing spinal lipoma with pAKT expression in a midline subcutaneous lipoma may identify dysraphism and tethered cord and prevent untoward patient outcome.

43 Silver In Situ Hybridization for the Rapid Assessment of MDM2 Amplification in Soft Tissue and Bone Tumours. Validation Based on an Audit of 192 Consecutive Cases Evaluated by Silver In Situ Hybridization and Fluorescence In Situ Hybridization

Gelareh Farshid¹, Sophia Otto¹, Maria Collis¹, Setha Napper¹, Mario Nicola²

¹Royal Adelaide Hospital, Adelaide, Australia, ²SA Pathology, Adelaide, Australia

Disclosures: Gelareh Farshid: None; Sophia Otto: None; Maria Collis: None; Setha Napper: None; Mario Nicola: None

Background: The discovery of almost invariable MDM2 amplification among atypical lipomatous tumours/well differentiated liposarcoma (ALT/WDL) and dedifferentiated liposarcoma (DDL) is incorporated into the contemporary diagnostic work up of fatty lesions. MDM2 amplifications are also found frequently in intimal sarcomas and in low grade osteogenic sarcoma. At present FISH is the reference test for MDM2 assessment. We are interested in evaluating Silver ISH for this purpose.

Design: Between October 2016 to May 2020, MDM2 status was assessed by both SISH and FISH in 192 soft tissue and bone lesions at our laboratory, including 77 (40.1%) core biopsies and 115 (58.9%) surgical specimens.

Results: The mean patient age was 61.0 years. The lesions location was the limbs: 75 (39.1%), intra-abdominal: 54 (28.1%) and other sites. After integration with FISH, the final diagnostic category was lipoma: 89 cases (46.4%), benign, reactive and inflammatory changes: 18 (9.4%), DDL: 21 (10.9%), ALT/WDL in 19 (9.9%), MDM2 amplified osteogenic sarcomas in 3 (1.6%), non-lipogenic sarcomas: 24 (12.5%), benign mesenchymal lesions: 14 (7.3%) and spindle carcinoma in 4 cases (2.1%).

SISH results were available overnight, or within 48 hours if repeat testing was required. FISH results were available within 2-5 weeks. The cost of SISH was one third of FISH.

Overall, FISH demonstrated MDM2 amplification in 44 cases (23.6%), no amplification was found in 144 cases (74.4%). Four cases (2.0%), all decalcified specimens, were non-diagnostic. SISH showed MDM2 amplification in 33 cases (17.2%), no amplification in 119 cases (62.0%) and indeterminate results due to poor signal in 40 (20.8%) cases. All 33 SISH amplified tumours were confirmed as amplified by FISH. Among 119 cases not amplified by SISH, 115 (95.0%) were confirmed as not amplified by FISH. Five cases (4.2%) were false negative by SISH but FISH showed MDM2 amplification, and one case (0.8%) was non-diagnostic by FISH. Among the 40 cases indeterminate with SISH, 6 (15.0%) were amplified by FISH, 31 (77.5%) were not amplified and 3 cases (7.5%) were non diagnostic by FISH. There were no clear differences in the performance of SISH on NCB versus surgical specimens. The overall performance indices of SISH are: sensitivity 75%, specificity 78.5%, positive predictive value 100% and negative predictive value 95.8%. The rate of inadequacy of SISH was 20.8%.

	FISH			Total
	Amplified	Non-Amplified	Failed	
SISH				
Amplified	33	0	0	33
Indeterminate	6	31	3	40
Non-Amplified	5	113	1	119
Total	44	144	4	192

Conclusions: A clearly amplified SISH result is clinically useful, particularly when concordant with the morphology. FISH may not be mandatory for these cases, improving laboratory efficiency. Non-amplified SISH results also provide early indications of the likely FISH findings, but there is a 4.2% chance of FISH being positive. At present the main drawback of SISH is the high rate of non-diagnostic tests. Optimisation of SISH signal detection, to reduce the proportion of indeterminate results is the current focus in this domain.

44 Immune Landscape Differences in Alveolar Soft Part Sarcoma and Undifferentiated Pleomorphic Sarcoma

Swati Gite¹, Luisa Solis Soto¹, Carmelia Noia Barreto¹, Ruth Salazar², Davis Ingram, Khalida Wani¹, Ignacio Wistuba¹, Wei-Lien (Billy) Wang¹, Alexander Lazar¹

¹The University of Texas MD Anderson Cancer Center, Houston, TX, ²IREN SUR, Lima, Peru

Disclosures: Swati Gite: None; Luisa Solis Soto: None; Carmelia Noia Barreto: None; Ruth Salazar: None; Davis Ingram: None; Khalida Wani: None; Ignacio Wistuba: None; Wei-Lien (Billy) Wang: None; Alexander Lazar: None

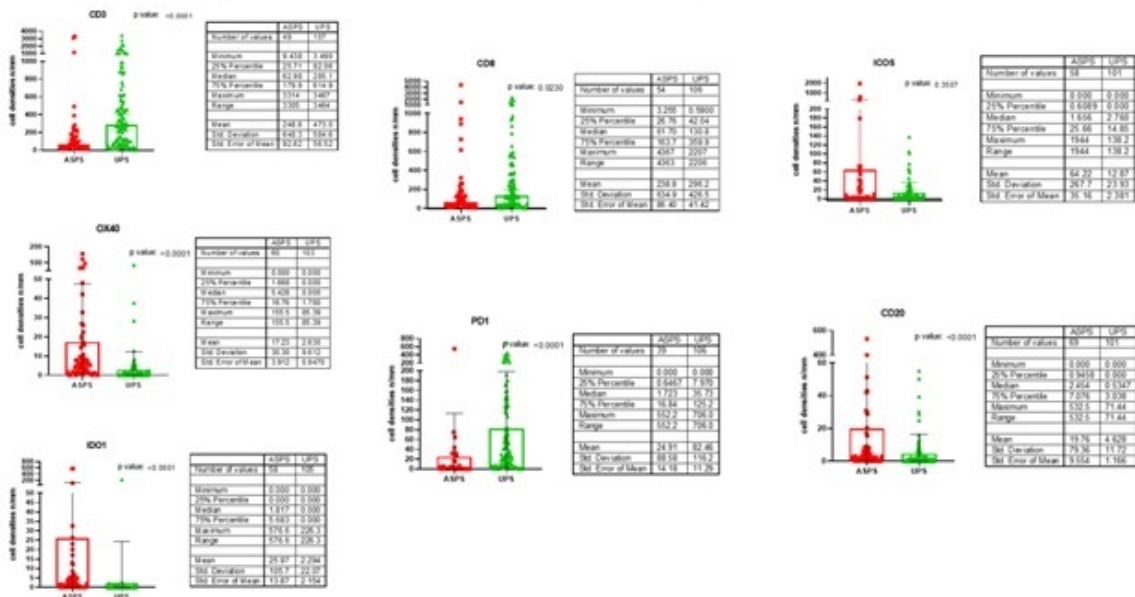
Background: Alveolar Soft Part Sarcoma (ASPS) and Undifferentiated Pleomorphic sarcomas (UPS) have different histological, genetic and epidemiological features. ASPS is rare malignant mesenchymal tumor characterized by unique ASPL-TEF3 fusion product while UPS are genetically complex sarcomas with high copy number alteration. Interestingly, both show relatively favorable response to immune checkpoint inhibitor therapy. Our aim is to define the immune infiltrate and expression of immune checkpoint biomarkers in a set of ASPS and UPS surgical resected tumor tissue and define the differences between these disparate sarcoma types.

Design: Formalin-fixed paraffin embedded (FFPE) tumor tissue from 64 patients with the diagnosis of ASPS and 107 patients with diagnosis of UPS were formatted into tissue microarrays (TMAs). We performed immunohistochemistry to quantify tumor infiltrating lymphocytes (TIL) (T cells: CD3 & CD8, B cells: CD20), monocytes-macrophages (CD163), NK cells (CD56), and immune cells positive for immune checkpoint (IC) (stimulatory: OX40 & ICOS; inhibitory: PD-L1, LAG3, IDO1, & PD1) and Adenosine Pathway (CD73 & CD39) biomarkers. We used digital image analysis to quantify immune cells with positive expression of these biomarkers and reported as cell density (n/mm²). PDL1, CD39 and CD73 was evaluated in malignant cells using standard microscopy and reported as percentage of tumoral expression.

Results: ASPS showed lower densities of both CD3+ and CD8+ cells as compared to UPS. CD20+ cell densities were higher in ASPS as compared with UPS. Higher cell densities of OX40, ICOS and IDO1 positive cells were observed in ASPS compared to UPS, while lower PD1 positive cell densities were found in UPS. (Figure 1). Expression of PD-L1, CD39 and CD73 in malignant cells of UPS was found in 19, 68 and 78% and that of ASPS was found in 28, 18 and 25 % respectively. (Cut-off ≥1%).

Figure 1 - 44

Figure 1: Comparison of ASPS and UPS biomarker Expression



Conclusions: In this study, we found that immune profiles of ASPS and UPS were significantly different. UPS have higher CD3+, CD8+ and PD1+ cell density and higher expression of biomarkers of adenosine pathway. ASPS have higher cell density of B cells, OX40, ICOS and IDO1 positive cells. These results suggest that different immune mechanisms are activated in this sarcoma subtype.

45 Pleomorphic Liposarcoma: A Series of 104 Cases with Emphasis on the Myxofibrosarcoma-Like Variant

Sandra Gjorgova Gjeorgjievski¹, Ivy John², Andrew Folpe³, Brian Rubin¹, Khin Thway⁴, Karen Fritchie¹
¹Cleveland Clinic, Cleveland, OH, ²University of Pittsburgh Medical Center, Pittsburgh, PA, ³Mayo Clinic, Rochester, MN, ⁴Royal Marsden Hospital, London, United Kingdom

Disclosures: Sandra Gjorgova Gjeorgjievski: None; Ivy John: None; Andrew Folpe: None; Brian Rubin: None; Karen Fritchie: None

Background: Pleomorphic liposarcoma (PLPS) is a highly aggressive sarcoma composed of variable numbers of pleomorphic lipoblasts admixed with undifferentiated pleomorphic sarcoma (UPS)-like areas. A significant number of cases harbor myxoid zones devoid of lipoblasts, reminiscent of myxofibrosarcoma (MFS) that may cause diagnostic confusion especially on core biopsy.

Design: PLPS biopsies and resection specimens were reviewed. Those with MFS-like morphology were defined by the presence of areas identical to conventional MFS, occupying at least 10% of the tumor volume. UPS-dominant and epithelioid PLPS were characterized by >50% UPS-like and epithelioid morphology, respectively.

Results: 104 total cases of PLPS occurred in 65M and 39F ranging from ages 18 to 93 years (median 64). Cases arose in the extremities (n=65), trunk (n=12), chest wall (n=9), head/neck (n=9), bone (n=4) and pelvis (n=3). Of those with known depth (n=73), 37 were intramuscular, 30 were subcutaneous and 6 arose in the dermis. Sizes ranged from 1 to 24.5 cm (median 7). Of cases with follow-up (n=71), 5 (7%) recurred and 17 (24%) metastasized. 50 cases (48%) contained a MFS-like component (31M, 19F; age range 18-93 years, median 62). When depth was assessable in this cohort (n=38), 19 were intramuscular and 18 were subcutaneous while 1 was centered in the dermis. MFS-like areas comprised 10 to 90% of the tumor volume (median 50%). Of those MFS-like PLPS with follow-up (39 of 50), 2 (5%) patients had local recurrence, and 8 (21%) had metastatic disease. 17 cases were UPS-dominant and 2 of 12 (17%) cases with follow-up metastasized, while 2 cases harbored epithelioid morphology, and 1 of 2 (50%) of those cases metastasized. None of the UPS-dominant or epithelioid PLPS recurred locally. 5 cases of MFS-like PLPS were misclassified as myxofibrosarcoma (n=4) or myxoinflammatory fibroblastic sarcoma (n=1) on initial biopsy while 3 PLPS were favored to represent UPS.

Conclusions: The percentage of MFS- and UPS-like histology PLPS varies widely, and such tumors are easily mistaken for conventional MFS or UPS. The distinction of such tumors from conventional MFS is particularly treacherous in the subcutis, where conventional MFS are common. The natural history of MFS-like PLPS appears to be roughly similar to that of other PLPS and more aggressive than conventional MFS. Those with MFS-like morphology seem to be at higher risk for local recurrence than UPS-dominant or epithelioid PLPS.

46 Patients with Concomitant Gout and Pseudogout (Calcium Pyrophosphate Dihydrate Disease) Demonstrate Unique Clinicopathologic Features Compared to Those with Only Gout

Sandra Gjorgova Gjeorgjievski¹, Josephine Dermawan¹, Scott Kilpatrick¹
¹Cleveland Clinic, Cleveland, OH

Disclosures: Sandra Gjorgova Gjeorgjievski: None; Josephine Dermawan: None; Scott Kilpatrick: None

Background: Gout is a crystal arthritide linked to chronic hyperuricemia, resulting in acute arthritis and chronic tophaceous disease. It is far more common in males, usually initially presenting in middle aged adults, and generally manifests in the digits of the feet and hands, especially the great toe. Calcium pyrophosphate dihydrate deposition disease (CPPD), also known as pseudogout, is a crystalline and metabolic arthritis, typically observed in the proximal large joints, especially the knees of elderly patients with osteoarthritis. Over the last several years, we

have rarely observed patients who had evidence of both gout and pseudogout within the same resected tissues. The incidence, significance, and clinicopathologic features of these patients have not been extensively analyzed.

Design: We retrospectively reviewed consecutive cases of pathologic specimens with a diagnosis of “gout” or “gouty tophi” between 11/1/2016 to 8/15/2020, evaluated by the authors, ultimately focusing on those examples that also had documented CPPD in the report. Clinicopathologic information including patient age (years), gender, site, and distribution of the crystals also were correlated. CPPD was easily identified by routine H&E staining; unstained slides confirmed the presence of polarizable needle shaped urate crystals for gout.

Results: A total of 161 cases of gout were confirmed (131 males; 30 females; ratio 4.4:1), with ages ranging from 14 to 99 years (median 67). 9 (5.5%) patients (6 males; 3 females; ratio 2:1) had evidence of both gout and CPPD crystal deposits within the same specimen; ages ranged from 48 to 91 years (median 74). Concomitant gout and pseudogout were more commonly associated with the upper extremities (total 5 [3, hands; 2, elbows]) than lower extremities (total 4, feet). The remaining 152 cases of gout not associated with CPPD occurred in 126 males; 27 females; ratio 4.7:1), ranging from 14 to 99 years (median 67). When gout occurred without CPPD, it was far more commonly seen in the lower extremities (107 cases) than in the upper extremities (40). The finding that combined gout/pseudogout was more commonly observed in the upper extremities was statistically significant (Mid-P exact test $P < 0.04838$). Deposits of CPPD were intimately associated with the gouty tophi, never being seen in the tissues outside of the tophaceous deposits, at times involving both soft tissue and bone. The volume of urate crystals always exceeded that of the calcium pyrophosphate crystals.

Conclusions: The presence of concomitant CPPD and gout is only rarely observed in pathology specimens, representing approximately 5.5% of all “resected” gout cases. Despite limited data, it appears that patients containing both gout and pseudogout are more likely to be female (although still more common in males) and have upper extremities involvement, compared to those patients with gout alone, who are far more likely to be male patients with lower extremity involvement. When present in patients with gout, CPPD crystals are intimately associated with the gout tophi.

47 Dedifferentiated Chondrosarcoma: How Much Really Counts?

Muhammad Hakim¹, Philippos Costa¹, Julio Diaz-Perez¹, Mohadese Behtaj¹, Jaylou Velez Torres¹, Elizabeth Montgomery¹, Andrew Rosenberg²

¹University of Miami Miller School of Medicine, Miami, FL, ²University of Miami Health System, Miami, FL

Disclosures: Muhammad Hakim: None; Philippos Costa: None; Julio Diaz-Perez: None; Mohadese Behtaj: None; Jaylou Velez Torres: None; Elizabeth Montgomery: None; Andrew Rosenberg: None

Background: Dedifferentiated chondrosarcoma is a highly malignant neoplasm with a dismal prognosis. This study investigates the relationship between the percent dedifferentiation and the outcomes of patients who underwent attempted curative resection.

Design: The databases of the participating institutions and consult files of one of the authors were queried for dedifferentiated chondrosarcoma. All patients with dedifferentiated chondrosarcoma who underwent resection whose slides were available for review to assess the percentage of the dedifferentiated component between the years 2012-2020 form the study cohort. Additional clinicopathological characteristics evaluated included patient demographics, size and location of tumor, tumor histological characteristics, resection margin status, treatment modalities, and outcomes to analyze prognostic factors. Progression-free-survival curves and hazard ratios were estimated using the Kaplan-Meier method and Cox proportional-hazards modeling.

Results: 17 of 90 patients fulfilled the study inclusion criteria. 10 (59%) patients were female and 7 were male with the mean age of 55 years (range 33-71) (Table 1). Femur (n=8, 47%) and ribs (n=6, 35%) were the most common sites. All dedifferentiated components were high grade and the percentage of dedifferentiation ranged from 1 – 90% (mean 25%) (Table 2). After resection, the 1-year progression-free survival rate was 65% (95% CI 41-89), with a median follow up of 24 months. One (6%) patient developed a local recurrence, and 8 (47%) patients developed distant metastases at a median interval of 14 months. The progression risk was higher when the dedifferentiated component was greater than 20% (HR: 6.0 95% CI 1-38; $P < 0.05$) (Figure 1). The mean progression-free survival was 28 months for patients whose tumors had less than 5% dedifferentiation, 26 months when the component ranged from 10-20%, and 10 months for patients with a dedifferentiated component over 20%. Of 9 patients in

whom the dedifferentiated component was less than 5%, 4 (44%) developed distant metastasis, to bone (2 patients) and lung (2 patients) and one (11%) experienced a local recurrence.

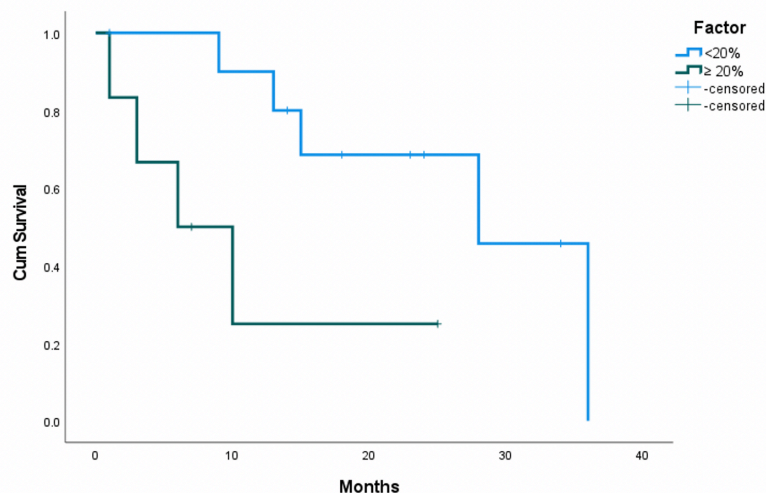
Table 1. Clinical characteristics and outcomes

Case number	Sex	Age (diagnosis)	Location	Size (cm)	% Dedifferentiated Tumor	Time to Progression (Months)	Progression after resection?	Outcome	Follow up time (Months)
1	F	70	Left Proximal Humerus	16.7	1%	NP	No	Alive	19
2	F	45	Right 9-10 Ribs	7	1%	15	Lung Metastasis	Alive	18
3	M	62	Left 3-5 Ribs	7.5	1%	NP	No	Alive	13
4	M	51	Right 4 Rib	10.4	2%	NP	No	Alive	34
5	F	71	Left Proximal Femur	14.5	2%	13	Bone Metastasis	LTFU	17
6	M	34	Left Tibia	7	3%	NP	No	Alive	25
7	F	53	Right 3 Rib	2.7	3%	9	Local Recurrence	Alive	25
8	M	54	Left 4-5 Ribs	15	5%	28	Bone Metastasis	Alive	55
9	F	33	Right 3 Rib	6	5%	36	Lung Metastasis	Alive	42
10	M	61	Left Scapula	8.5	10%	NP	No	LTFU	2
11	M	39	Right Femur (Acetabulum)	2.6	15%	NP	No	Alive	25
12	F	60	Left Distal Femur	7.5	40%	1	Lung Metastasis	Alive	24
13	M	67	Left Distal Femur	8	50%	10	Lung metastasis	Dead	42
14	F	59	Right Femur (Acetabulum)	8.2	50%	NP	No	Alive	11
15*	F	71	Right Femur	4	66%	NP	No	Alive	26
16*	F	55	Proximal Tibia	11	80%	3	Lung Metastasis	LTFU	5
17	F	83	Right Femur	7.3	90%	6	Lung Metastasis	Alive	16

*Post-neoadjuvant chemotherapy. LTFU: Lost to follow up. NP: No progression

Figure 1 - 47

Figure 1



Kaplan–Meier Estimates of the Recurrence-free Survival by percentage of the dedifferentiated component. Data from patients who did not have progression were censored and marked by a tick.

Conclusions: The prognosis of dedifferentiated chondrosarcoma correlates with the percentage of dedifferentiation in the tumor. Patients whose tumors have greater than 20% dedifferentiation have the worse prognosis. Importantly even patients with tumors with $\leq 5\%$ dedifferentiation behave in an aggressive fashion.

48 HEY1 is a Sensitive and Specific Marker in the Diagnosis of Mesenchymal Chondrosarcoma

Alexandra Isaacson¹, Jason Hornick², Andrew Bellizzi¹

¹University of Iowa Hospitals & Clinics, Iowa City, IA, ²Brigham and Women’s Hospital, Harvard Medical School, Boston, MA

Disclosures: Alexandra Isaacson: None; Jason Hornick: None; Andrew Bellizzi: None

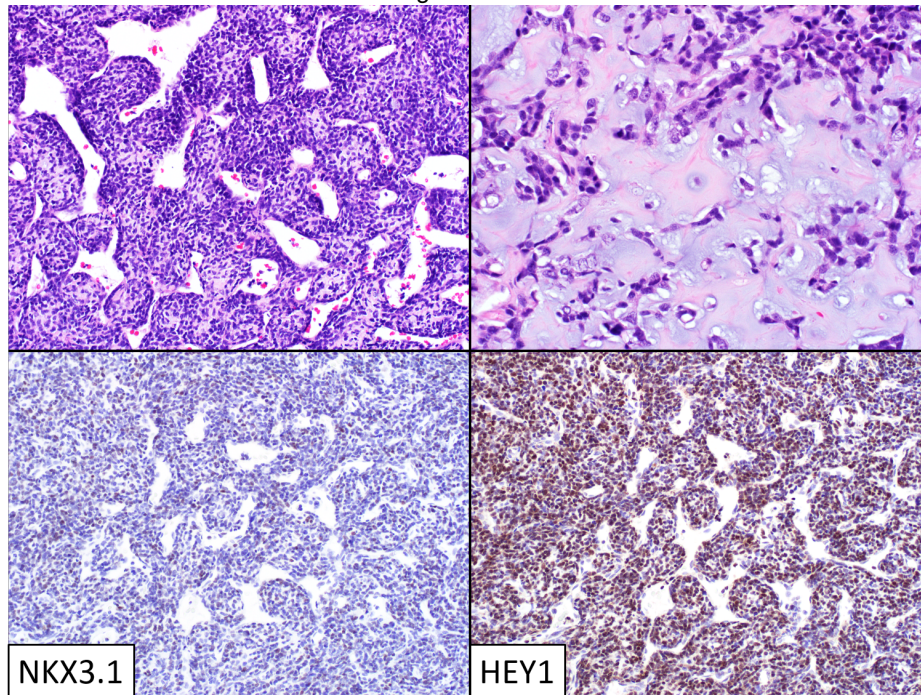
Background: Mesenchymal chondrosarcoma (MC) is an undifferentiated sarcoma characterized by primitive small round blue cells with intermixed islands of mature hyaline cartilage. In the absence of a mature cartilage component, MC is morphologically indistinguishable from other small round blue cell (SRBCT) tumors. NKX3.1 was recently suggested by Yoshida *et al* to be a sensitive and specific marker for MC (12/12 MCs positive); however, these results were not corroborated in a follow-up study by Fletcher and colleagues (0/25 MCs positive). We studied NKX3.1 in a limited number of MCs and found staining to be positive, though weak and patchy. This prompted a search for a more robust diagnostic marker.

MC is driven by a recurrent *HEY1-NCOA2* fusion that is considered diagnostic for this entity. We initially investigated NCOA2 as a potential diagnostic marker due to its distal location in the fusion and found it to be sensitive and strong, though non-specific among SRBCT. Conversely, HEY1 nuclear staining appears to be both sensitive and specific biomarker for MC.

Design: A polyclonal antibody to the N-terminus of HEY1 was optimized for immunohistochemistry (IHC) in a *HEY1-NCOA2* next-generation sequencing-confirmed MC. Staining was performed on 30 archival MCs from 22 patients (mainly as whole sections) and tissue microarrays of diagnostic mimics: 23 rhabdomyosarcomas (RMS; 14 embryonal, 9 alveolar), 10 olfactory neuroblastomas, 13 synovial sarcomas, 12 Ewing sarcomas, 9 lymphoblastic lymphomas, 35 Wilms tumors, 67 neuroblastomas, 6 desmoplastic small round cell tumors, and 2 *BCOR*-rearranged sarcomas. NKX3.1 IHC was performed on 8 MCs. Intensity (0-3+) and extent (0-100%) of expression were evaluated, and an H-score was calculated.

Results: Nuclear positivity for HEY1 was present in 28 of 30 MCs at a mean (median) H-score of 186 (225). 26 tumors were diffusely moderate to strongly positive (2-3+, 25%-100%). Two cases showed weak positivity (1+, 5-40%), and two cases were HEY1-negative. Four RMS (3 alveolar, 1 embryonal) showed focal HEY1 nuclear positivity (range of H scores= 2-22.5); all other tumors showed cytoplasmic or no HEY1 staining. HEY1 was, thus, 93% sensitive and 98% and specific. At an H-score threshold >30, the sensitivity and specificity were 90% and 100%. NKX3.1 demonstrated focal weak to moderate positivity in 7 of 8 MCs (1-3+, rare cells to 35%).

Figure 1 - 48



Conclusions: Nuclear staining for HEY1 is sensitive and specific for MC, particularly useful in suspected cases that lack the classic biphasic morphology with mature cartilaginous elements. The presence of cytoplasmic staining in non-MC tumors also suggests that the HEY1-NCOA2 fusion leads to HEY1 nuclear translocation in MC. We demonstrate consistent focal but weak positivity for NKX3.1 in MC and suspect that reported discrepancies in NKX3.1 staining may be assay-dependent.

49 CSF1 Chromogenic in situ Hybridization (CISH) in the Diagnosis of Benign and Malignant Tenosynovial Giant Cell Tumors (TGCT)

Judith Jebastin Thangaiah¹, Justin Koeplin¹, Andrew Folpe¹
¹Mayo Clinic, Rochester, MN

Disclosures: Judith Jebastin Thangaiah: None; Justin Koeplin: None; Andrew Folpe: None

Background: Rearrangements of the *CSF1* (Colony Stimulating Factor-1) locus at 1p13.3 are central to the pathogenesis of TGCT of both localized (LTGCT) and diffuse (DTGCT) types, and have been demonstrated in a small number of studied malignant examples (MTGCT) as well. *CSF1* rearrangements are thought to occur in synoviocytes, result in *CSF1* mRNA and protein overexpression, and lead to a massive influx of *CSF1R*-expressing non-neoplastic macrophages and osteoclast-like giant cells. Very recently, CISH for *CSF1* mRNA has been shown to be potentially useful in the diagnosis of TGCT, although only a relatively small number of cases have been studied. We studied a large series of well-characterized TGCT and non-TGCT *CSF1* mRNA expression using CISH.

Design: Using a commercially available CISH kit (Advanced Cell Diagnostics, Biotechne) and the RNAscope® VS Universal HRP Assay (Brown), we examined *CSF1* mRNA expression on formalin-fixed, paraffin-embedded whole tissue sections from 28 TGCT (13 LTGCT, 12 DTGCT, 2 MTGCT) and 5 leiomyosarcomas, 5 squamous cell

carcinomas, 5 prostate adenocarcinomas, 4 mesotheliomas, 3 urothelial carcinomas, 1 thymic carcinoma, and 1 angiomyolipoma. We also evaluated tissue microarray(TMA) constructs from Pantomics normal TMA (MNO341-34 human normal tissue from all organ systems), Pantomics tumor TMA (MTU391 -TCC bladder, HCC liver, RCC-kidney, adenocarcinoma from stomach, colon, pancreas, ovary, uterus, prostate, lung, and breast, SqCC from lung, skin, and uterus, melanoma and lymphoma), Pantomics melanoma TMA (MEL961- 8 skin, 8 nevus, 4 BCC, 4 SCC, 38 skin melanoma, 4 ocular melanoma, 6 anal melanoma, 24 metastatic melanoma in lymph nodes).

Results: CSF1 CISH was positive in all TGCT (28/28, 100%). The positivity was limited to large, eosinophilic cells morphologically compatible with synoviocytes. The number of CSF1-positive cells was markedly elevated in MTGCT. CSF1 mRNA expression was rare in non-TGCT, and was observed only in a small number (3/145, 2%) and included leiomyosarcoma (2/5, 40%), pulmonary SCC (1/6, 16%), and pulmonary small cell carcinoma (1/6, 16%). The sensitivity and specificity of CSF1 CISH in the diagnosis of TGCT were 100% and 98% respectively.

Figure 1 - 49

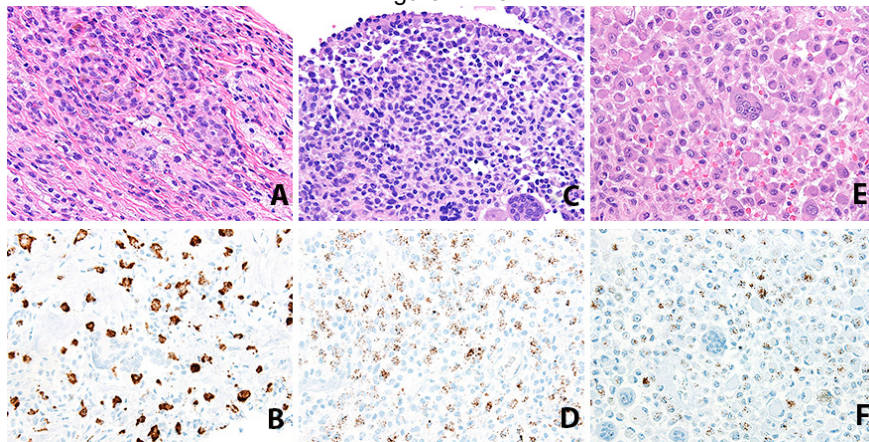
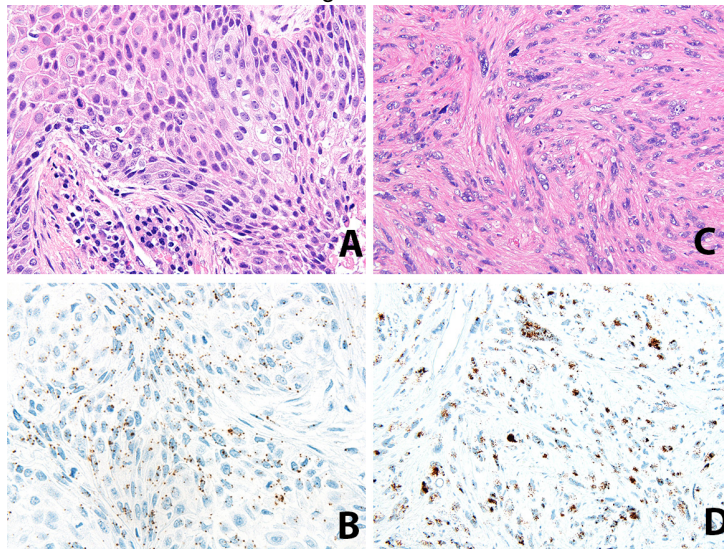


Figure 2 - 49



Conclusions: CISH for CSF1 mRNA ISH is highly sensitive and relatively specific marker of TGCT of all types, including malignant examples. The presence of very large number of CSF1-positive cells in MTGCT supports our prior hypothesis that MTGCT represent true malignancies of synoviocytes. Demonstration of CSF1 mRNA expression may be valuable in the diagnosis of challenging TGCT, in particular giant cell-poor examples and extra-articular DTGCT, and may be predictive of response to the specific CSF1 inhibitor pexidartinib. We have also confirmed prior observations of CSF1 mRNA expression in leiomyosarcomas.

50 Adult Rhabdomyosarcoma: Clinical and Pathologic Characterization of 53 Cases

Erica Kao¹, Eleanor Chen¹

¹University of Washington, Seattle, WA

Disclosures: Erica Kao: None; Eleanor Chen: None

Background: Rhabdomyosarcoma (RMS) is well studied in children and adolescents. In adults, however, it is rarer and the clinical behavior and pathologic findings are not well characterized. In this study, we seek to determine if clinical behavior of adult RMS differs by histologic subtype, and if there are any unique features of these tumors specific to adults. In this study, we retrospectively review 53 RMS cases and correlate histologic subtype as well as other parameters with clinical outcomes.

Design: We searched our institutional archives for cases diagnosed as RMS between 2000 and 2020. All available histologic slides and diagnoses were reviewed. Demographic characteristics, clinical history, histologic and pathologic features, as well as outcomes (recurrence and metastasis) measured by event-free survival were

Subtype	n	M:F	Mean Age (yrs)	Mean Size (cm)	EFS (months)	ST (months)
PRMS	29	2.2:1	61.6	8.5	12.1	34.7
ERMS	9	0.8:1	42	10.6	4.3	9.3
ARMS	11	1.2:1	40.2	3.4	17.3	29.3
SS	4	3:1	45.8	11.9	22.1	30.2

recorded.

Results: We reviewed 53 cases of RMS in adults [29 pleomorphic (PRMS)], 9 embryonal (ERMS), 11 alveolar (ARMS), 4 spindle cell/sclerosing (SS)]. There were 20 female patients and 33 male patients (M:F ratio of 1.7:1). Patient ages ranged from 21 to 88 years (mean 52.5). Classic and unique histologic features for each subtype were identified. All cases were positive for Desmin and MyoD or Myogenin on immunohistochemistry. Tumor size ranged from 1 to 29 cm (mean 9.4 cm) and the distribution of anatomic location was head and neck 30% (16/53), trunk 21% (11/53), extremities 34% (18/53), and viscera 15% (8/53). 59% of PRMS were located in the extremity (17/29), 56% of ERMS were in viscera (5/9), 91% of ARMS (10/11) and 50% of SS (2/4) were in the head and neck. Clinical follow up information was available for 48 patients. Recurrence or metastatic disease was recorded in 35 patients. Overall, an event free survival (EFS), ranged from 0 to 62.6 months (mean 12.8 months; PRMS: 12, ERMS: 4.2, ARMS: 17.3, SS: 22.1 months) and an overall survival time (ST), ranging from 0.9 months to 139.5 months (mean 33 months; PRMS: 34.7, ERMS: 9.2; ARMS: 29.3; SS: 30.2). By log-rank test, there was no significant difference in EFS and ST among RMS subtypes. Metastatic disease by imaging or biopsy occurred in the lung (n=14), liver (n=3), brain (n=5), and bone (n=5).

Summary of parameters by subtype

Figure 1 - 50

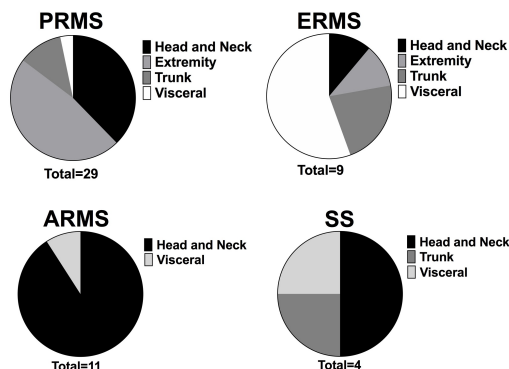


Figure 1. Summary of tumor location by subtype

Figure 2 - 50

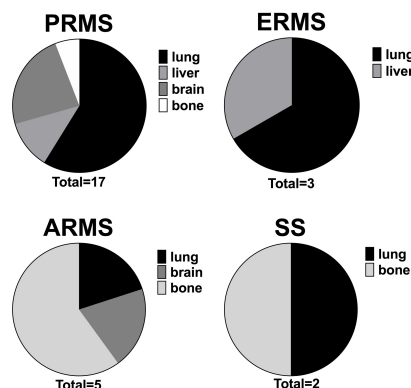


Figure 2. Location of metastasis by subtype

Conclusions: Certain RMS subtypes in adults show a predilection for the extremity (PRMS), visceral organs (ERMS), or the head and neck (ARMS). RMS is an aggressive neoplasm in adults, associated with a poor prognosis for event-free survival and overall survival time regardless of subtype.

51 Tumor Mutation Burden and UV Signature Mutation Index Help in Distinguishing Malignant Peripheral Nerve Sheath Tumors from Desmoplastic Melanomas

Arivarasan Karunamurthy¹, Cihan Kaya¹, Ijeuru Chikeka¹, Bruce Leckey¹, Rana Naous¹, Jonhan Ho¹, Ivy John¹

¹University of Pittsburgh Medical Center, Pittsburgh, PA

Disclosures: Arivarasan Karunamurthy: None; Cihan Kaya: None; Ijeuru Chikeka: None; Bruce Leckey: None; Rana Naous: None; Jonhan Ho: None; Ivy John: None

Background: Malignant peripheral nerve sheath tumor (MPNST), a highly aggressive soft-tissue sarcoma, tends to arise in the deep soft tissues of the proximal upper and lower extremities and trunk. MPNSTs, especially the superficial variants, share many histological and immunohistochemical similarities to spindle cell melanoma (SCM)/desmoplastic melanoma (DM) and may lead to misdiagnosis. Both neoplasms show recurrent and increased frequency of NF1 mutations and hence are genetically indistinguishable based on the mutational profile alone.

Design: We analyzed publicly available TCGA whole exome data sets of 21 DM/SCMs and 16 MPNSTs for tumor mutation burden (TMB) using our customized OncoPrint TMB formula. We calculated UV signature mutation burden as CT index (percentage of C>T and CC>TT transitions against total number of mutations) among these data sets. In addition, we also performed NGS based DNA sequencing using OncoPrint V3 (0.29Mb) assay on 9 in-house MPNST cases and calculated TMB and CT index using the above customized formula.

Results: Both cohorts (MPNST & SCM/DM) showed recurrent mutations in NF1, TERT promoter region and RAS genes. We identified a low number of tumor mutation burden in TCGA MPNST cohort (median 3.2, range 0–13.7) as well as in-house MPNST cohort (mean 5.2, range 2–11). In contrast, the TCGA SCM/DM cohort showed high TMB (mean 23.6, range 0–62.8). Statistical analysis using t-test showed very significant (p 0.000035) TMB difference between the MPNST & DM cohorts. Similarly, the whole exome CT index was high in SCM/DM cohort (mean 42%, range 15–49%) and significantly different (p 0.00013) compared to MPNST TCGA (mean 13%, range 7–21%) and reproducibly low in-house MPNST cohort (mean 15%, range 9–18%) performed on targeted OncoPrint panel.

Conclusions: Superficial MPNSTs pose diagnostic difficulties due to shared morphological, immunohistochemical and genetic features with SCM/DMs. Many cutaneous melanomas are associated with increased sun/ultraviolet radiation exposure and tend to carry high mutation burden with UV specific signatures. We report that tumor mutation burden and CT mutation index are distinctively different between these neoplasms and can serve as useful markers in the diagnosis of challenging MPNST cases.

52 Rapidly Destructive Arthropathy of the Hip: Pathologic Findings in a Case Series

Lester Layfield¹, Julia Crim¹

¹University of Missouri, Columbia, MO

Disclosures: Lester Layfield: None

Background: Rapidly destructive arthropathy of the hip (RDAH) refers to noninfectious arthropathy which causes extensive femoral head bone destruction. It has been described in the literature using a variety of diagnostic criteria, but it remains a poorly defined entity, and much is unknown regarding its prevalence, etiology and histologic appearance.

Design: This study was IRB approved and HIPAA compliant. Cases of RDAH diagnosed at our institution between July 1, 2015 and December 31, 2019 were identified from a free text search of the radiology report data base. Imaging studies and pathology specimens were retrospectively reviewed. Histopathologic features were analyzed

to document characteristic features of RDAH and determine if significant morphologic differences existed between RDAH and osteoarthritis and avascular necrosis.

Results: Twenty femoral heads were identified where there was 25% or greater destruction of the femoral head in the absence of infections, congenital disease, osteonecrosis (avascular necrosis), and inflammatory arthritis. Documented pre-existing conditions included Intra-articular corticosteroid injection, prior hip trauma and insufficiency fracture. Destructive arthropathy was characterized pathologically by loss of articular cartilage and bone end plate, a vascularized fibromyxoid change of the marrow, subarticular aggregates of necrotic bone fragments, increased numbers of osteoclasts, increased trabecular bone destruction and granuloma-like aggregates. Not all cases demonstrated all pathologic features but loss of articular cartilage and absence of the bone end plate were nearly universally present (Table 1). Increased numbers of osteoclasts and granulomas were uncommon findings.

	Absence of Cartilage	Absence of Bone end plate	Bone Fragments	Bone Remodeling	Osteoclasts	Granuloma	Fibromyxoid Stroma
Number of Cases (%)	20 (100%)	19 (95%)	14 (70%)	17 (85%)	7 (35%)	3 (15%)	14 (70%)

Conclusions: The histologic findings were distinctive allowing separation of RDAH from avascular necrosis and osteoarthritis (OA). RDAH lacks the large wedge-shaped zone of osteonecrosis characteristic of avascular necrosis. RDAH contains one or more foci of necrotic bone fragments, increased numbers of osteoclasts and areas of bone remodeling not characteristic of OA. We postulate that a variety of pre-existing conditions (including insufficiency fracture) set in motion a cascade of tissue factors which lead to bone destruction.

53 Expanding the Molecular Genetic Spectrum of Adult Bone and Soft Tissue Fibrosarcomas: An Institutional Experience

Bruce Leckey¹, Ivy John¹, Abigail Wald¹, Rana Naous¹

¹University of Pittsburgh Medical Center, Pittsburgh, PA

Disclosures: Bruce Leckey: None; Ivy John: None; Abigail Wald: None; Rana Naous: None

Background: Fibrosarcomas, once comprising the majority of unclassifiable spindle-cell sarcomas, are now regarded as a diagnosis of exclusion constituting <1% of adult sarcomas. This shift in fibrosarcoma diagnosis incidence is likely due to novel defining genetic alterations. Prompted by an index report of *NTRK3* fusion in adult-type fibrosarcomas by Yamazaki et al., bone/soft tissue tumors diagnosed as fibrosarcoma at our institution were evaluated, using NGS RNA Fusion analysis and DNA/RNA sequencing, for the presence of novel gene alterations, including *NTRK*-related fusions, in an attempt to expand the genetic spectrum of fibrosarcomas and identify therapeutically targetable cases.

Design: Institutional archives were searched for cases diagnosed as “fibrosarcoma” involving bone/soft tissue from 2000-present. Thirty cases were identified, 6 were excluded (2 metastatic disease, 3 recurrent disease and 1 re-excision of residual disease). Of the remaining 24 cases, 13 cases had formalin fixed paraffin embedded tissue blocks available for molecular testing. RNA for 12 cases was extracted from the neoplasms and subjected to NGS RNA Fusion analysis and 1 case was sent for DNA/RNA sequencing (FoundationOne®).

Results: Clinicopathologic results, including the presence/absence of gene fusions or molecular aberrations, are summarized in Table 1. At the time of diagnosis, the mean age was 57 (range 14-88) with a male to female ratio of 1.6:1. Locations included soft tissue of the lower extremity (3), upper extremity (2), trunk (3), and pelvis (2), bone (2), and lymph node (1). Tumor grade included low-grade (5), intermediate-grade (1), and high-grade (7). Of the 13 cases, 1 case demonstrated a *FNDC3B-PIK3CA* gene fusion, and 1 case demonstrated a *BRAF (G469A)* mutation and loss of *CDKN2A/B*.

Case	Age	Gender	Site	Diagnosis	Molecular Testing	Genetic Alteration
1	68	M	Right Posterior Thigh	Low-Grade Fibrosarcoma	NGS RNA Fusion analysis	Negative
2	85	M	Right Inguinal Lymph Node	High-Grade Inflammatory Fibrosarcoma	NGS RNA Fusion analysis	Negative
3	88	F	Right Forearm	High-Grade Fibrosarcoma	NGS RNA Fusion analysis	FNDC3B-PIK3CA fusion
4	67	F	Right Knee	Low-Grade Fibrosarcoma	NGS RNA Fusion analysis	Negative
5	66	M	Penis	Low-Grade Fibrosarcoma	NGS RNA Fusion analysis	Negative
6	48	M	Paraspinal Muscle/ L2-S1	High-grade Fibrosarcoma	NGS RNA Fusion analysis	Negative
7	60	F	Left Lower Arm	High-Grade Fibrosarcoma	NGS RNA Fusion analysis	Negative
8	14	M	Anterior Mandible	High-grade Fibrosarcoma	NGS RNA Fusion analysis	Negative
9	51	M	Right Chest Wall	High-Grade Fibrosarcoma, Post Radiation	NGS RNA Fusion analysis	Negative
10	58	F	Right Rectus Muscle	Low-Grade Fibrosarcoma	NGS RNA Fusion analysis	Negative
11	43	M	Left Middle Turbinate	Low-Grade Fibrosarcoma	NGS RNA Fusion analysis	Negative
12	30	M	Right Pelvis	High-Grade Fibrosarcoma	NGS RNA Fusion analysis	Negative
13	63	F	Right Lower Extremity	Intermediate-Grade Fibrosarcoma	DNA/RNA sequencing (FoundationOne®)	<i>BRAF</i> (G469A) mutation, <i>CDKN2A/B</i> loss

Conclusions: Two of 13 (15%) cases diagnosed as fibrosarcoma at our institution over the past 20 years demonstrated specific molecular aberrations, including 1 case with *FNDC3B-PIK3CA* gene fusion and 1 case with *BRAF* (G469A) mutation and loss of *CDKN2A/B*. *NTRK*-related gene fusions were not identified. The significance of such molecular aberrations in the setting of fibrosarcoma is not clear, and future studies are needed to establish whether these findings carry clinicopathologic significance. Alternatively, our data suggests that bone/soft tissue fibrosarcomas rarely harbor *NTRK*-related gene fusions; however, it may still be clinically advantageous to keep evaluating for these therapeutically targetable gene fusions.

54 Differential Expression of Immune Related Genes in the Components of Dedifferentiated Chondrosarcoma by RNA Sequencing

Bruce Leckey¹, Rebekah Belayneh¹, Rebecca Watters¹, Kurt Weiss¹, Anette Duensing², Uma Chandran¹, Alexander Chang¹, Vishal Soman¹, David Osei Hwedieh¹, Karen Schoedel³

¹University of Pittsburgh Medical Center, Pittsburgh, PA, ²UPMC Hillman Cancer Center, Pittsburgh, PA, ³UPMC Presbyterian Hospital, Pittsburgh, PA

Disclosures: Bruce Leckey: None; Anette Duensing: None; Vishal Soman: None; Karen Schoedel: None

Background: Dedifferentiation in chondrosarcoma (CS) is associated with poor survival and therapeutic options are limited. The possibility for emerging immune therapies applied to CS represents an alternative to surgical resection. We attempt to understand the differential expression of immune related genes in matched dedifferentiated (DD) and well differentiated (WD) components of DDCS.

Design: 8 DDCS were identified in the institutional archives. H&E slides corresponding to WD and DD areas of the tumors were circled and 10 um thick FFPE sections were cut, deparaffinized and RNA was extracted by standard methods. The yield was checked and samples were submitted for RNA sequencing. 3 cases had been previously sequenced by Truseq stranded total RNA. These were excluded from pathway analysis due to batch effect. 5 cases were subjected to RNA Exome and SMART sequencing. Data analysis was performed using Edge R 4.0 and pathway/network analysis was achieved through Qiagen IPA. The GO category 0050776 immune gene list was interrogated in conjunction with the RNA sequencing data. A subset of genes was selected based on network relevance and expression level. Statistical significance was set at <0.05 (right tailed Fisher's Exact test).

Results: Dedifferentiated components of DDCS demonstrated increased expression of genes related to activation of B and T lymphocytes and granulocytes, phagocytosis of phagocytes and degranulation. At the same time, DDCS showed greater cytotoxicity of lymphocytes, NK cells and cytotoxic T cells, p<0.05.

Gene	DDCS	WDCS
NKG2D	Increased	Decreased
KLRC4-KLRK1/KLRK1	Increased	Decreased
ULBP3, ULBP1	Increased	Decreased
B2M	Increased	Decreased
HLAB	Increased	Decreased
ICOSLG	Increased	Decreased
CD300LG	Decreased	Increased
BCL6	Decreased	Increased
TremL4	Decreased	Increased

Conclusions: The immune environment of DDCS is complex. In the DD component there is increased expression of several genes involved in immune regulation as compared to the WD component. Both activators and suppressors of immune mediation by the tumor were observed, potentially representing therapeutic targets.

55 The Immune Microenvironment of Solitary Fibrous Tumors

Nolan Maloney¹, Davis Ingram, Khalida Wani¹, Elizabeth Demicco², Wei-Lien (Billy) Wang¹

¹The University of Texas MD Anderson Cancer Center, Houston, TX, ²University of Toronto, Toronto, Canada

Disclosures: Nolan Maloney: None; Davis Ingram: None; Khalida Wani: None; Elizabeth Demicco: None; Wei-Lien (Billy) Wang: None

Background: Solitary fibrous tumor (SFT) is a fibroblastic mesenchymal tumor characterized by a *NAB2-STA76* fusion that can arise in virtually any anatomic site. Most SFTs behave in a clinically benign fashion and are cured by a complete excision. However, a minority of patients develop local recurrences and/or distant metastases, and therapeutic options for patients with metastatic disease are limited. Currently, immunotherapy is being explored as a possible treatment for sarcomas. We sought to characterize the immune microenvironment in a large series of SFTs to evaluate whether immune checkpoint-related therapies could be beneficial.

Design: Unstained slides were prepared from tissue microarray consisting of 116 formalin-fixed paraffin embedded solitary fibrous tumors of various sites. Immunohistochemical studies were performed using an autostainer: CD8 (1:100, C8/144B), CD20 (1:1400, L-26), CD163 (1:100, 10D6), PD-L1 (Dako 22C3), PD-1 (1:100, MRQ-22), ICOS (1:100, D1K2T), LAG3 (1:100, D2G40), and IDO1 (1:100, D5J4E). Both tumoral and number of immune infiltrate expression / 1 mm diameter core were assessed. For CD8 and CD163, the number of positive immune cells per core was categorized using a three-tiered scoring system (CD8: 0=none, 1=1-50 cells/core, 2=51-100 cells/core, 3=>100 cells/core; CD163: 0=none, 1=1-50 cells/core, 2=51-200 cells/core, 3=>200 cells/core).

Results: All cases contained CD163+ macrophages (116/116, mean score: 1.5), 83% contained CD8 positive lymphocytes (94/113, mean score: 1.2), 58% showed vascular IDO1 expression (63/108), 18% contained CD20 positive lymphocytes (15/112), 9% contained LAG3 positive lymphocytes (9/104), 5% contained ICOS positive

lymphocytes (5/105), 2% contained PD-1 positive lymphocytes (2/92), and no cases showed expression of PD-L1 (0/109). 2 cases showed rare tumoral ICOS positivity and 3 cases had lymphocytes with IDO1 positivity. IDO1 positive vasculature was less commonly seen in tumors of meningeal origin (7/21, 33%) versus elsewhere (54/72, 75%).

Conclusions: Similar to other reported sarcomas, macrophages and CD8 positive lymphocytes are the predominant immune cells present in SFTs, with macrophages being present in every case examined, while B-lymphocytes were identified in a minority of cases. While SFTs lack expression of the most common immune checkpoint markers, IDO1 was found expressed in the vasculature in many cases, was more prevalent in tumors of non-meningeal origin and may play an immunosuppressive role for these tumors. As there is no effective chemotherapeutic regimen, these findings overall suggest that exploration of immunotherapy targeting IDO1 or macrophage pathways in aggressive SFTs warrants further exploration.

56 STAT6 is a More Sensitive and Specific Immunohistochemical Marker than CD34 for Diagnosing Solitary Fibrous Tumor with Round Cell Morphology

Sambit Mohanty¹, Ruhani Sardana², Shivani Sharma³, Ekta Jain³, Aditi Dewan⁴, Preeti Diwaker⁵, Shefali Chopra⁶

¹AMRI Hospital, Chandigarh, India, ²AMRI Hospital, ³Core Diagnostics, Gurgaon, India, ⁴Core Diagnostics, Gurugram, India, ⁵UCMS and GTB Hospital, Delhi, India, ⁶Keck School of Medicine of USC, Los Angeles, CA

Disclosures: Sambit Mohanty: None; Ruhani Sardana: None; Shivani Sharma: None; Ekta Jain: None; Aditi Dewan: None; Preeti Diwaker: None; Shefali Chopra: None

Background: Solitary fibrous tumor (SFT) is a fibroblastic tumor with thin walled vasculature and NAB2- STAT6 gene rearrangement. This can occur at any anatomic site including soft tissue and visceral locations. Most tumors have spindle cell morphology with fewer cases with round cell morphology described. Tumors with round cell morphology especially on the needle core biopsy can be diagnostic challenging as SFT is not often thought of as a differential diagnosis for the round cell tumors. We sought to analyze the percentage of tumors with round cell morphology and expression of CD34 and STAT6 in such tumors.

Design: All patients with the diagnosis of SFT both soft tissue and visceral locations were retrieved by pathology database of 3 institutions. Diagnosis on all patients included in this study was confirmed by strong and diffuse nuclear STAT6 expression on immunohistochemistry (IHC). Clinicopathologic data was collected, histology and IHC slides were reviewed, and follow-up information wherever available was recorded. Fluorescence in situ hybridization (FISH) for STAT6 was performed in 16 and multiplexed sequencing assay in 2 patients.<

Results: Forty- five specimens from 34 patients were retrieved. There were 22 patients with both biopsy and resection, 5 patients with only biopsy, and 18 with only resection specimens. The median age was 57 years (23-78 years) and male: female ratio was 3:1. 18 patients had tumors which were spindle cell, 8 had pure round cell morphology, and 8 were mixed. 19 tumors were from the soft tissue and 15 were from the viscera. The tumors ranged from 1 cm to 25 cm (median=6.9 cm). 16 patients had malignant SFT with 11 patients being on systemic therapy with follow up. Metastasis and recurrence were seen in 7 and 2 patients, respectively, while 2 patients with follow up for a year having no recurrence or metastasis so far. Of the remaining 18 patients, 13 were at low risk and 5 at intermediate risk for progressive disease. Of the 16 malignant patients, 8 had pure round cell and 4 each had spindle and mixed morphology. 4 additional patients were of mixed morphology (two each were of intermediate risk and low risk for progressive disease) (Figure1). Complete CD34 loss was seen in 9 of the malignant patients; 8 of which were of pure round cell and one spindle cell/pleomorphic histology. Partial CD34 loss was observed in 4 mixed morphology and 2 spindle cell morphology in the malignant group. Of the low and intermediate risk tumors, CD34 loss was seen in one spindle cell and two mixed morphology. 7 of 16 patients exhibited STAT6 break-apart FISH positivity. Multiplexed sequencing assay was positive for NAB2-STAT6 fusion in 2 malignant patients.

Figure 1 - 56

Table 1. Tumor histology and STAT6 and CD34 expression pattern in Solitary Fibrous Tumor.

Tumor Histology/Cell Type	STAT6	CD34
Malignant round cell (8)	Positive (8; 100%)	Negative (8; 100%)
Malignant spindle cell (4)	Positive (4; 100%)	Positive (1; 25%) Negative (1; 25%) Partial loss (2; 50%)
Malignant mixed morphology (4)	Positive (4; 100%)	Negative (1; 25%) Loss in the round cells (3; 75%)
Low and intermediate with round cell (0)	Not applicable	Not applicable
Low and intermediate with spindle cell (14)	Positive (14; 100%)	Positive (11; 79%) Negative (2; 14%) Partial loss (1; 7%)
Low and intermediate with mixed morphology (4)	Positive (4; 100%)	Positive (1; 25%) Negative (2; 50%) Loss in the round cells (1; 25%)

Conclusions:

1. Round cell SFTs especially the malignant ones tend to lose CD34, highlighting the diagnostic utility of adding STAT6 to the IHC panel when trying to classify round cell tumors.
2. As observed in earlier studies, FISH is less sensitive than STAT6 IHC for diagnosing SFT.
3. CD34 loss is more often seen in malignant tumors.

57 Immunohistochemical Detection of SSX Fusion-Specific Proteins: Novel, Highly Specific Monoclonal Antibodies to Distinguish Synovial Sarcoma from Its Histologic Mimickers

Sara Moradi¹, Jonathan Earle¹, Srini Mandavilli¹, Richard Cartun², Pamela Newcomb³

¹Hartford Hospital, ²Hartford Hospital, Hartford, CT, ³Hartford Hospital, Hartford Pathology Associates, Hartford, CT

Disclosures: Sara Moradi: None; Srini Mandavilli: None; Richard Cartun: None

Background: SS18-SSX refers to oncogenic fusion proteins in synovial sarcoma (SS) that result from the fusion of the SS18 gene on chromosome 18 with SSX1, SSX2, and, less commonly, SSX4 on the X chromosome. SS is a rare, malignant soft-tissue tumor that occurs in young patients. SS harbors a fusion involving the SS18 gene that leads to detectable expression of the residues surrounding the SS18-SSX fusion site. Our goal was to determine if the commercially-available (Cell Signaling Technology, Danvers, MA) rabbit monoclonal antibodies (mAbs) directed against the SS18-SSX fusion-site protein (clone E9X9V) and to the carboxyl terminal end of the SSX fusion partner (clone E5A2C) were exclusively expressed in SS compared to other soft tissue tumors with similar morphologic features.

Design: We performed immunoperoxidase (IP) testing using both clones on formalin-fixed, paraffin-embedded tissue sections from 11 cases of FISH-proven SS, in addition to 17 soft tissue tumors with similar morphology to SS. We also included 7 cases of malignant melanoma that could be included in the differential diagnosis of poorly differentiated SS.

Results: Our study showed that both rabbit mAbs showed diffuse, strong nuclear expression in 100% of the 11 cases of SS tested. No expression was observed with either antibody in the 17 soft tissue tumors studied that could histologically mimic SS. These cases included four cases of malignant peripheral nerve sheath tumor, two cases of

Ewing sarcoma, one case of sarcoma with BCOR genetic alteration, two cases of solitary fibrous tumor, one case of malignant solitary fibrous tumor, two cases of undifferentiated sarcoma, one case of leiomyosarcoma, one case of alveolar rhabdomyosarcoma, one case of embryonal rhabdomyosarcoma, and one case of malignant ossifying fibromyxoid tumor.

Among the seven melanoma cases studied, three showed some immunoreactivity for one or both clones as follows: one metastatic melanoma showed weak, focal positivity for the E9X9V clone, one primary spindle cell melanoma showed partial positivity for the both clones and two metastatic melanoma showed focal positivity for the E5A2C clone. However, all melanoma cases had been confirmed using IP testing with routine melanoma markers (S-100, HMB45, Melan-A, and SOX-10).

Conclusions: Our findings show that the SS18-SSX and SSX rabbit mAbs used in our study are highly sensitive and specific for synovial sarcoma, with melanoma being a possible pitfall.

58 Clinicopathological Prognostic Factors of Dedifferentiated Liposarcoma: A Study of 127 Primary Resected Cases

Taro Mori¹, Yuichi Yamada¹, Izumi Kinoshita¹, Kenichi Kohashi¹, Hidetaka Yamamoto¹, Yoshinao Oda¹
¹*Kyushu University, Japan*

Disclosures: Taro Mori: None; Yuichi Yamada: None; Izumi Kinoshita: None; Kenichi Kohashi: None; Hidetaka Yamamoto: None; Yoshinao Oda: None

Background: Dedifferentiated liposarcoma (DDLs) is a malignant lipomatous neoplasm composed of atypical lipomatous tumor/well differentiated liposarcoma (ALT/WDLs) component and low- or high-grade sarcomatous component. Previous studies reported that DDLs might appear various histological types of dedifferentiated components. However, there were very limited studies about their significance in prognosis. Herein, we reviewed large series of primary DDLs from both clinical and histological viewpoints and examined the significance of histological types.

Design: We retrieved 127 primary DDLs cases from the record of our institution from 1974 to 2019. All the cases were diagnosed by using *MDM2* immunohistochemistry and/or fluorescent in situ hybridization and histologically reviewed by two pathologists. Clinical data about sex, age, dedifferentiated size, location and outcome (tumor-related death, local recurrence and distant metastasis) were collected. Histologic evaluation items were as follows; histological grade, mitotic count, necrosis, FNCLCC grade, ALT/WDLs component and heterologous differentiation. We also generated overall survival (OS), metastasis-free survival (MFS) and recurrence-free survival (RFS) curves by using Fisher's exact test and Kaplan-Meier method with log-rank test. The statistical analyses were performed for three groups; 1. all cases, 2. internal DDLs (n=82) and 3. external DDLs (n=45).

Results: The clinical and histological data were summarized in the Table. Statistical results were as follows;

1. All cases: The RFS of internal DDLs was significantly shorter than that of external DDLs ($p=0.0033$). The cases with distant metastasis showed significantly shorter OS ($p<0.0001$), but local recurrence did not significantly relate to either OS or MFS. Histologically, the OSs with high-grade components and epithelioid variant were significantly shorter ($p=0.0389, 0.0475$).
2. Internal DDLs: Distant metastasis was significantly relative to shorter OS ($p=0.0010$). However, the relationship between local recurrence and OS/MFS did not reach statistical significance. Histologically, higher mitotic count was significantly associated with shorter OS and MFS ($p=0.0015, 0.0178$). Epithelioid variant was also significantly associated with shorter OS ($p=0.0085$).
3. External DDLs: Although local recurrence significantly relate to neither OS nor MFS, distant metastasis was significantly relative to shorter OS ($p=0.0103$). Histologically, necrosis was significantly associated with shorter OS and MFS ($p=0.0131, 0.0269$). The cases with high-grade variants showed significantly shorter OS ($p=0.0110$).

Characteristics	Case	n (%)			p-value		
		OS	RFS	MFS			
Sex							
	Male	84 (66.1)	0.9908	0.3209	0.5633		
	Female	43 (33.9)					
Age (median 66 y.o.)							
	<65 y.o.	60 (47.2)	0.4595	0.2862	0.2022		
	>65 y.o.	67 (52.8)					
Dedifferentiated size (median 10 cm)							
	<10 cm	59 (46.5)	0.2876	0.1622	0.4756		
	>10 cm	55 (43.3)					
Location							
	Internal (intraperitoneal, intrapleural and paratesticular regions)	82 (64.6)	0.5837	0.0033	0.8998		
	External (other than the above)	45 (35.4)					
Tumor-related death							
	+	33 (26.0)	N.A.	<0.0001	<0.0001		
	-	91 (71.7)					
Local recurrence							
	+	62 (48.8)	0.1579	N.A.	0.9203		
	-	56 (44.1)					
Distant metastasis							
	+	32 (25.2)	<0.0001	0.2934	N.A.		
	-	93 (73.2)					
Histological grade							
	Low grade	95 (74.8)	0.0389	0.0905	0.2538		
	High grade	30 (23.6)					
Mitotic count							
	Low (<10/10HPFs)	83 (65.9)	0.0009	0.5156	0.0087		
	High (>10/10HPFs)	44 (34.1)					
Necrosis							
	+	55 (43.3)	0.0131	0.7215	0.0354		
	-	72 (56.7)					
FNCLCC grade							
	G2	92 (72.4)	0.0014	0.6553	0.0110		
	G3	35 (28.6)					
ALT/WDLS component							
	+	67 (52.8)	0.3753	0.8832	0.9567		
	-	60 (47.2)					
Lipoblastic diff.							
	+	24 (18.9)	0.9519	0.6146	0.7106		
	-	103 (81.1)					
Smooth muscular diff.							
	+	19 (15.0)	0.3871	0.1111	0.4976		
	-	104 (81.9)					
Osteo-/chondrogenic diff.							
	+	14 (11.0)	0.8640	0.8733	0.1690		
	-	113 (89.0)					
Epithelioid variant							
	+	10 (7.9)	0.0475	0.3024	0.7616		
	-	117 (92.1)					

Conclusions: It was suggested that epithelioid variant may be one of the prognostic factors of DDLS. Moreover, it was demonstrated that internal DDLS tended to recur in comparison with external DDLS, whereas local recurrence may not influence the prognosis of DDLS.

59 "Neuroendocrine-Like Neoplasm": Clinicopathologic Analysis of 23 Cases of a Distinctive Soft Tissue Tumor with Metastatic Potential, Recurrent CTNNB1 Mutations and a Predilection for Truncal Locations

David Papke¹, Lynette Sholl¹, Brendan Dickson², Christopher Fletcher¹

¹Brigham and Women's Hospital, Boston, MA, ²Mount Sinai Health System, Toronto, Canada

Disclosures: David Papke: None; Lynette Sholl: *Grant or Research Support*, Genentech; Brendan Dickson: *Grant or Research Support*, Illumina; Christopher Fletcher: None

Background: The spectrum of epithelioid soft tissue neoplasms continues to expand and includes PEComa, epithelioid schwannoma and emerging entities such as sarcomas with *GLI1* alterations. Here, we describe a previously unrecognized entity, provisionally termed "neuroendocrine-like neoplasm" (NEN). NEN is a rare, distinctive tumor of uncertain lineage with a predilection for paravertebral deep soft tissue of adults.

Design: 23 cases from the consultation archives of one of the authors were studied to determine the clinicopathologic characteristics of NEN. Next-generation sequencing was performed on 7 tumors using targeted DNA (6/7) and RNA (6/7) sequencing.

Results: 15 patients (65%) were male. Age at presentation ranged from 32–81 years (median: 65 yr). Paravertebral soft tissue was the most common location (15 tumors; 65%), followed by upper back (2 tumors), posterior head (2), gluteal (1) and inguinal (1) regions, thigh (1) and orbit (1). Tumor size ranged from 2–19 cm (median: 6.35 cm).

NEN is composed of sheets and nests of epithelioid cells with pale eosinophilic cytoplasm and highly monomorphic, round nuclei with fine chromatin very reminiscent of neuroendocrine tumors. Psammomatous calcifications were present in 8 tumors (35%), and extracellular round eosinophilic secretions were identified in 9 (39%). Lymphovascular invasion was present in 5/18 tumors (28%). Myxoid stroma and metaplastic ossification were identified in one case each. Immunohistochemistry (IHC) demonstrated at least focal positivity for β -catenin (19/22 tumors; 86%), S-100 (9/22; 41%), desmin (3/8; 38%) and CD34 (2/8; 25%). IHC was uniformly negative for neuroendocrine and epithelial markers, including synaptophysin (21 tumors), chromogranin (19), INSM1 (4), pan-K (16), CAM5.2 (13), AE1/AE3 (6), EMA (20) and E-cadherin (13).

DNA sequencing detected *CTNNB1* point mutations in all sequenced tumors: D32H, S33C, S33F, S37A, S37C and S37F. RNA sequencing was negative for gene fusions in all sequenced tumors.

Clinical follow-up was available for 16 patients so far (70%; range: 0.2–20 yr; median: 3.2 yr). 5/16 tumors (31%) recurred, and 3/16 (19%) metastasized to lung. No patient died of disease as yet.

Conclusions: NEN is a low-grade malignant neoplasm with a predilection for paravertebral soft tissue. Based on its negativity for epithelial proteins and positivity for desmin and CD34, NEN is likely mesenchymal in nature.

60 Integrated Next Generation Sequencing and Gene Expression Analysis of 10 Pleomorphic Rhabdomyosarcoma Cases Reveals Potential Drivers and Druggable Targets

Vera Paulson¹, Zachary Chelsky², Eleanor Chen²

¹University of Washington Medical Center, Seattle, WA, ²University of Washington, Seattle, WA

Disclosures: Vera Paulson: None; Zachary Chelsky: None; Eleanor Chen: None

Background: Pleomorphic rhabdomyosarcoma (PRMS) is a rare and aggressive adult sarcoma, with an overall survival of less than 2 years for the majority of patients. Treatment options for PRMS are limited, and most patients do not respond to conventional chemotherapy and radiation. Molecular features of PRMS have been poorly characterized. To date, cytogenetic and comparative genomic hybridization (CGH) studies of small PRMS cohorts have demonstrated complex structural alterations and few recurrent regional gains and losses. Thus, there remains an urgent need for more comprehensive molecular profiling to both understand disease pathogenesis and to identify potentially actionable targets for treatment purposes with the goal of improved survival.

Design: 10 PRMS resection cases were retrieved from institutional archives for molecular studies. In brief, genomic DNA from formalin fixed and paraffin embedded (FFPE) tumor tissue blocks was evaluated using Oncoplex, a next generation sequencing (NGS) assay designed to detect single nucleotide variants, copy number alterations, select structural rearrangements, microsatellite instability, and tumor mutational burden in 340 genes related to cancer treatment, prognosis, and diagnosis. In parallel, RNA was extracted from matched tumor and normal FFPE samples of 6 cases for multiplex targeted sequencing using the Nanostring nCounter tumor signaling 360 panel, which targets 770 genes involved in tumor biology, immune evasion, and microenvironment remodeling.

Results: OncoPlex identified alterations in cell cycle regulators (TP53, CDKN2A, CDKN2B and CDK4) in 90% of cases, the Receptor Tyrosine Kinase(RTK)/RAS/MAPK/AKT pathways (NF1, KRAS, PTEN, FGFR1 and AKT3) in 80% of cases, genes involved in telomere maintenance (TERT) in 40% of cases, chromatin remodeling (ATRX, HIST1H3B, CREBBP and KMT2D) in 25% of cases, and DNA repair (SLX4 and MSH3) in 20% of cases, as well as the WNT signaling pathway (GNAS) in 10% of cases. Microsatellite instability was absent in all cases, and tumor mutational burden was predominantly low. Analysis of gene expression profiling results revealed up-regulation of many of the same pathways in at least a subset of the samples analyzed, including the RTK/MAPK, AKT/PIK3C/mTOR, and Wnt pathways. Increased Hedgehog and JAK/STAT pathway signaling was also observed.

Conclusions: Our integrated analysis of PRMS using a combination of DNA and RNA sequencing platforms has demonstrated alterations in pathways that represent not only drivers of disease pathogenesis, but potentially druggable targets (e.g. CDK4/CDKN2A/B, RTK- MAPK and AKT/PIK3C/mTOR pathways).

61 Immunohistochemical Evaluation of SS18-SSX and SSX Expression in Synovial Sarcomas and Mimickers with Previous FISH Analysis for SS18 Rearrangement

Raheel Rizwan¹, Jianhui Shi¹, Angela Bitting¹, Haiyan Liu¹, Fan Lin¹

¹Geisinger Medical Center, Danville, PA

Disclosures: Raheel Rizwan: None; Jianhui Shi: None; Angela Bitting: None; Haiyan Liu: None; Fan Lin: None

Background: Diagnosis of synovial sarcoma (SS) can be challenging because of overlapping histologic features with a range of other tumors and a lack of highly specific immunohistochemical (IHC) markers. Cytogenetic or molecular genetic testing for t(X;18)(p11;q11) translocation is considered the “gold standard” to confirm the diagnosis. A recent study reported 2 highly sensitive and specific antibodies, SS18-SSX and SSX, with 95% and 100% sensitivity, and 100% and 96% specificity, respectively (Baranov E et al. Am J Surg Pathol 2020;44:922-933). In this study, we investigated the expression of these 2 novel antibodies in 38 consecutive tumor cases which were suspicious for SS and had previous fluorescence in situ hybridization (FISH) analysis for SS18 rearrangement.

Design: Fifty-four consecutive tumor cases with previous FISH testing for SS18 rearrangement were identified from our pathology archives. Thirty-eight cases were found to have available tissue blocks, including 14 cytologic samples/cell blocks and 24 surgical specimens. Using the Leica Bond III staining platform, IHC detection of SS18-SSX (E9X9V; 1:1600; Cell Signaling) and SSX (E5A2C; 1:800; Cell Signaling) expression was performed on these 38 cases, including 12 cases of SS (9 monophasic, 2 biphasic and 1 poorly differentiated variant) and the mimickers listed in Table 1. The results were recorded as negative (no nuclear staining), 1+ (<25 tumor cell nuclear stained), 2+ (26-50%), 3+ (51-75%), and 4+ (76-100%).

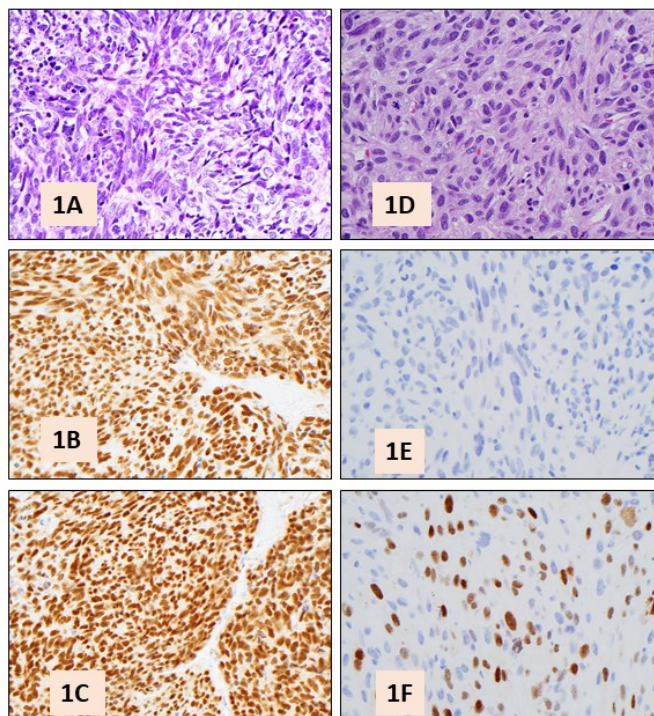
Results: All 12 SS cases were diffusely positive (3+ or 4+) for both SS18-SSX and SSX. All 26 cases FISH-negative for SS18 rearrangement were negative for SS18-SSX. However, 3 of the 26 FISH-negative cases were focally positive for SSX, including 1 sarcomatoid carcinoma, 1 dedifferentiated liposarcoma, and 1 spindle cell sarcoma. Figure 1 shows a representative case of SS to be positive for SS18-SSX and SSX and the dedifferentiated liposarcoma to be positive for SSX and negative for SS18-SSX.

Table 1. Final Diagnosis of 26 cases with Negative FISH Analysis for SS18 Rearrangement

Diagnosis	No. of Cases
Sarcomatoid carcinoma/undifferentiated carcinoma	5
Dedifferentiated liposarcoma	3
High grade undifferentiated sarcoma	3
Small round cell sarcoma	3
Nephroblastoma	2
MPNST	2
Spindle cell sarcoma	2
Sclerosing epithelioid fibrosarcoma	1
Proximal type epithelioid sarcoma	1
Myxoid-round cell liposarcoma	1
Perineurioma	1
Ossifying fibromyxoid tumor	1
Benign cellular fibrohistiocytoma	1

MPNST - Malignant peripheral nerve sheath tumor

Figure 1 - 61



Figures 1A-1F showing a synovial sarcoma (1A) positive for SS18-SSX (1B) and SSX (1C) and a dedifferentiated liposarcoma (1D) negative for SS18-SSX (1E) and focally positive for SSX (1F). Both cases are from cell blocks.

Conclusions: Our data support those of the above publication, that both SS18-SSX and SSX are highly sensitive and specific markers to confirm the diagnosis of SS, and IHC can potentially replace FISH or molecular testing in the detection of SS18 rearrangement. Both antibodies generate robust nuclear signals; therefore, it is particularly useful for small biopsy/cytologic samples suspicious for SS. Caution should be taken since the antibody to SSX can be focally positive in rare other tumors.

62 Juvenile Xanthogranuloma in Children and Adults: A 30-Year Single-Center Experience

Behzad Salari¹, Louis Dehner²

¹Washington University in St. Louis, St. Louis, MO, ²Washington University School of Medicine, St. Louis, MO

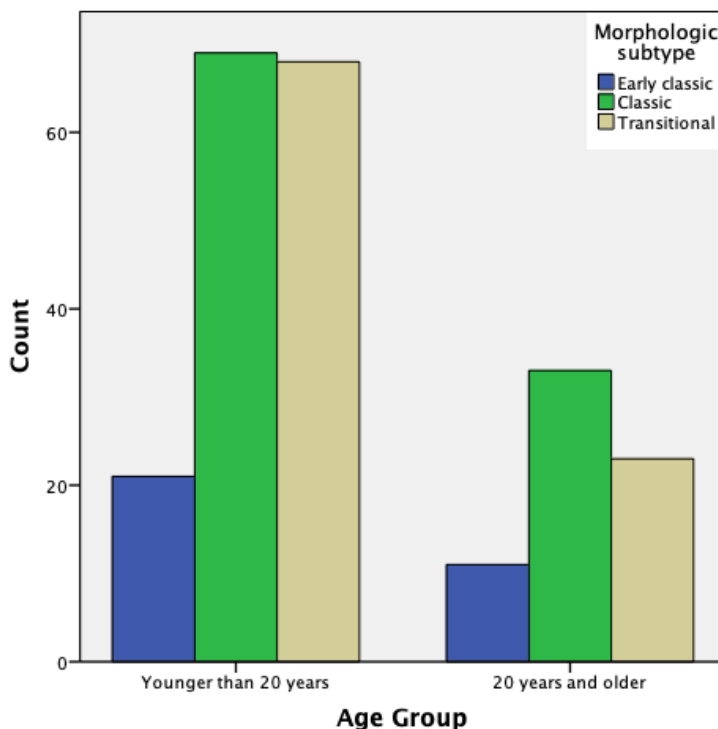
Disclosures: Behzad Salari: None; Louis Dehner: None

Background: Juvenile xanthogranuloma (JXG), the most common form of non-Langerhans histiocytosis. Its cell of origin, etiology and pathogenesis are not fully understood. We aimed to provide an update on histologic and immunophenotypic profile of this uncommon entity.

Design: A retrospective review of all the cases with the pathologic diagnosis of “xanthogranuloma” was performed from our archives from 1989 to 2019.

Results: A total of 525 patients with 547 JXG lesions were identified with the median age of 4.5 years and a male predominance (M:F ratio 1.3:1). The lesions occurred most frequently on the head and neck (40.8%). Cutaneous lesions comprised 76.8% cases and of the remaining extracutaneous lesions 15.7% were within soft tissue. The most common non-soft tissue, extracutaneous lesions were in the brain (2.6%), and lungs (1.8%). Morphologic subtype included 14.2% early classic (EJXG), 45.3% classic (CJXG), and 40.5% transitional JXG (TJXG) (Figure 1). Multinucleated giant cells, either Touton or non-Touton, were most frequently present in CJXG followed by TJXG. Mitosis was rare (<1/10 high-power field) among different subtypes. We found an association between morphologic subtype and lymphocytic infiltrates ($P = 0.036$), and presence of Touton or non-Touton giant cells ($P < 0.001$ for both) but not for mitotic count ($P = 0.105$) or eosinophilic infiltrates ($P = 0.465$). Additionally, there was an association between age group and presence of non-Touton giant cells ($P = 0.012$) but not Touton cells ($P = 0.127$) or mitotic count ($P = 0.220$). We demonstrated immunophenotypic expression of the lesion regardless of age or morphologic subtype: Factor XIIIa 192/204 (94.1%), CD11c 75/77 (97.4%), CD4 82/84 (97.6%), CD68 200/201 (99.5%), CD163 15/15 (100%), CD1a 1/110 (0.9%), S-100 48/152 (31.6%), CD31 15/21 (71.4%), and vimentin 104/105 (99.0%).

Figure 1 - 62



Conclusions: We described histologic and immunophenotypic profile of JXG and its associations in different age groups and evolutionary stages. Considering sensitivity and specificity rates, we suggest that a combination of CD11c, CD4, CD1a and either CD163 (preferred) or CD68 stains can provide a better diagnostic yield when evaluating for differential diagnosis.

63 NTRK-Rearranged Spindle Cell Neoplasm: A Clinicopathologic and Molecular Study of 9 Cases Revealed Two Novel Fusion Genes in One of the Largest Institution of Southwest China

Changle Shi¹, Lijuan Yin¹, Xin He², Yan Qiu², Huijiao Chen², Min Chen², Zhang Zhang², Hongying Zhang²
¹West China Hospital, Sichuan University, Chengdu, China, ²West China Hospital, Sichuan University

Disclosures: Changle Shi: None; Lijuan Yin: None; Xin He: None; Yan Qiu: None; Huijiao Chen: None; Min Chen: None; Zhang Zhang: None; Hongying Zhang: None

Background: *NTRK*-rearranged spindle cell neoplasm represents an emerging group of rare soft tissue tumors defined by molecular means. To the best of our knowledge, there has been no series report about this tumor in Chinese population in English literature to date.

Design: Between 2009 and 2020, 9 *NTRK*-rearranged spindle cell neoplasm of children was included (age≤22y). The clinicopathologic features of all cases were reviewed. Immunohistochemical staining was carried out for pan-TRK, TRK-A, H3K27me3, SOX-10, S-100 protein and CD34. *NTRK1/2/3* rearrangements/fusion were performed by fluorescence in situ hybridization (FISH) and next generation sequencing (NGS) (425 gene), and validated by reverse transcription polymerase chain reaction (RT-PCR).

Results: This series of cases accounted for 0.05% of all the pediatric spindle cell tumor during the same period, including 5 males and 4 females. The median age was 4 years old (range, 1 mo-22 y). The tumors occurred mainly in the trunk (6/9, 67%), followed by extremities (3/9, 33%). The median tumor size was 4 cm (range 1-7cm). Histologically, 2 cases displayed as lipofibromatosis-like neural tumor (LPF-NT); 3 cases exhibiting low-grade fibrosarcoma-like or malignant peripheral nerve sheath tumor (MPNST)-like morphology, were classified as Fédération Nationale des Centres de Lutte Contre le Cancer (FNCLCC) grade 1; 3 cases showing spindle cells proliferating in solid pattern with variable amounts of collagen fiber, displaying MPNST-like features, were classified as FNCLCC grade 2; 1 case showing myxofibrosarcoma-like morphology, was classified as FNCLCC grade 3. Immunohistochemically, 9/9(100%) cases were CD34, pan-TRK and TRK-A positive, SOX-10 negative and H3K27me3 intact, whereas S-100 protein expression was identified in 7/9(78%) cases. Genetically, *NTRK1* rearrangements were detected by FISH in all cases. NGS identified and RT-PCR confirmed *NTRK1* fusions with variety of partner genes (n=8). We detected two novel fusions, *CPSF6-NTRK1* (n=1, 12.5%) and *SQSTM1-NTRK1* (n=1, 12.5%), in addition to the common types of *LMNA-NTRK1* (n=4, 50%) and *TPM3-NTRK1* (n=2, 25%). All patients underwent mass resection, two of them had amputation. Clinical follow-up was available in 7/9 cases (range 9-70 mo, median 41 mo). Five patients developed local recurrence (range 6-46 mo, median 13 mo), and 2 of them suffered distant metastasis.

Conclusions: This study presents the first series of *NTRK*-rearranged spindle cell neoplasm in Chinese children. We identified two novel fusion genes, which has not been reported in mesenchymal tumors, although one has been reported in single case of lung cancer. Well understanding the clinicopathologic features and molecular pathogenesis are helpful in selecting patients for TRK-targeted therapy.

64 Mesenchymal Neoplasms of Salivary Glands: An Institutional Experience of 66 Cases

Jaylou Velez Torres¹, Julio Diaz-Perez¹, Ernesto Martinez Duarte², Mohadese Behtaj¹, Muhammad Hakim¹, Elizabeth Montgomery¹, Carmen Gomez-Fernandez¹, Andrew Rosenberg³
¹University of Miami Miller School of Medicine, Miami, FL, ²University of Nebraska Medical Center, Omaha, NE, ³University of Miami Health System, Miami, FL

Disclosures: Jaylou Velez Torres: None; Julio Diaz-Perez: None; Ernesto Martinez Duarte: None; Mohadese Behtaj: None; Muhammad Hakim: None; Elizabeth Montgomery: None; Carmen Gomez-Fernandez: None; Andrew Rosenberg: None

Background: Salivary gland neoplasms are uncommon, and most show epithelial differentiation. Mesenchymal neoplasms of the salivary gland are rare, and the incidence ranges from 1.9% to 5%. To increase our understanding of salivary gland mesenchymal neoplasms, we reviewed our institutional experience.

Design: A retrospective search for mesenchymal neoplasms of salivary glands from the pathology archives of our institution from 2004-2020 period and consultation files of one of the authors was performed. The clinical data were obtained from available medical records, and the histological slides and ancillary studies were retrieved and reviewed.

Results: We identified a total of 66 cases that form the study cohort. Thirty-four patients were male, and thirty-two patients were female, with a mean age of 48 years (range, 7 months -79 years), and the male to female ratio was 1:.94. Sixty of sixty-six tumors were benign and included: 37 (56%) lipomas, 9 (14%) hemangiomas, 7 (11%) schwannomas, 2 (3%) neurofibromas, 2 (3%) lymphangiomas, 2 (3%) solitary fibrous tumors, and 1 (1%) myofibroma. Six of sixty-six were malignant and included: 3 (5%) adamantinoma-like Ewing sarcomas, 2 (3%) malignant peripheral nerve sheath tumors (MPNST), and 1 (1%) malignant solitary fibrous tumor. The involved sites included: parotid gland (53), parapharyngeal space (5), submandibular gland (5), minor salivary gland (2), and sublingual gland (1). Sixty-five patients underwent surgical resection. One patient with lymphangioma manifested a recurrence/persistence a week post-surgery. One patient with a parotid hemangioma developed post-operative numbness, and another patient developed chronic postauricular pain after surgery. Two patients with MPNST and one patient with adamantinoma-like Ewing sarcoma underwent neoadjuvant chemoradiation and were disease-free after treatment. The remaining 37 patients with available follow-up that ranged from 7 days-156 months (mean, 21 months) had a favorable outcome and were disease-free after treatment. The clinicopathologic data are summarized in table 1.

Table 1. Clinicopathologic Features of Mesenchymal Neoplasms of the Salivary Gland

Gender	Age (years)	Location	Diagnosis	Size (cm)
M	18	Right parotid	Intraparotid lipoma	3.0
M	62	Right parotid	Spindle cell lipoma	4.0
M	55	Parapharyngeal space mass	Lipoma	10.0
F	42	Right parotid	Intraparotid lipoma	3.0
F	66	Left parotid	Lipoma	6.5
F	48	Left parotid	Intraparotid lipoma	2.0
F	65	Right parotid	Lipoma	4.0
M	55	Right parapharyngeal space	Lipoma	3.0
F	47	Deep parotid	Lipoma	4.5
M	26	Left parotid	Lipoma	5.4
M	63	Right Parotid	Fibrolipoma	4.0
M	44	Right parotid	Lipoma	1.2
M	56	Left parotid	Lipoma	3.5
F	68	Right parotid	Lipoma	3.5
F	56	Right parotid	Lipoma	6.0
M	70	Right parotid	Lipoma	6.5
M	64	Left parotid	Lipoma	3.5
F	36	Right parotid	Lipoma	6.5
F	19	Left parapharyngeal space	Fibrolipoma	7.9
M	64	Parotid	Lipoma	5.2
F	46	Right parotid	Lipoma	4.0
M	55	Right parotid	Intraparotid lipoma	3.0
M	65	Left anterior parotid	Fibrolipoma	1.4
M	48	Right parotid	Lipoma	3.0
F	51	Left anterior parotid	Spindle cell lipoma	1.2
F	51	Right parotid	Lipoma	2.0
M	63	Left parotid	Intraparotid lipoma	5.7
M	63	Lip minor salivary gland	Pleomorphic lipoma	1.0
M	64	Right parotid	Lipoma	NA
M	59	Right parotid	Lipoma	2.0
F	67	Left submandibular gland	Lipoma	8.9
M	59	Right parotid	Lipoma	3.0
M	50	Right parotid	Lipoma	4.0
M	46	Left parotid	Lipoma	3.0
M	53	Left parotid	Lipoma	3.5
M	43	Right parotid	Lipoma	6.0
M	53	Right parotid	Schwannoma	6.4
F	40	Parapharyngeal space mass	Plexiform neurofibroma	3.4
M	54	Right parotid	Schwannoma	0.9
F	45	Parapharyngeal space mass	Schwannoma	NA

F	15	Left parapharyngeal space	MPNST	6.7
F	43	Right parotid	Schwannoma	NA
F	29	Left neck mass within parotid sheath	Schwannoma	2.5
F	53	Parotid mass	Schwannoma	3.9
F	36	Right parotid	Schwannoma	8
M	28	Left parotid	Neurofibroma	NA
F	12	Left parotid	MPNST	NA
F	40	Left parotid	Adamantinoma-like Ewing Sarcoma	2.4
F	21	Submandibular gland	Adamantinoma-like Ewing Sarcoma	5
F	79	Left parotid	Adamantinoma-like Ewing Sarcoma	2
M	59	Tail of parotid	Hemangioma	2.9
F	64	Right parotid	Hemangioma	3
F	46	Right parotid	Venous hemangioma	1.6
F	66	Right parotid	Cavernous hemangioma	NA
M	14	Left sublingual gland	Cavernous and capillary hemangioma	3.5
F	41	Left submandibular gland	Hemangioma	1.5
F	63	Right parotid	Venous hemangioma	2.5
M	31	Submandibular gland	Capillary hemangioma	NA
M	70	Right parotid	Hemangioma	3
F	12	Submandibular gland	Lymphangioma	1
M	1	Right parotid	Lymphangioma	5.2
M	60	Buccal mucosa (minor salivary gland)	Solitary fibrous tumor	1.5
F	57	Left parotid	Solitary fibrous tumor	3.2
F	72	Left parotid	Malignant Solitary Fibrous Tumor	7.0
M	7 months	Left parotid	Myofibroma	3.8

Abbreviations: NA: Not available; MPNST: Malignant peripheral nerve sheath tumor.

Conclusions: Mesenchymal neoplasms of salivary gland are rare, and awareness of their development is important for adequate diagnosis. The mainstay of treatment is surgical excision, with the extent determined by tumor type. Adjuvant therapy is reserved for high-grade sarcomas and may be given in a neoadjuvant or adjuvant setting.

65 NTRK1 Rearranged Mesenchymal Tumor: Clinicopathologic, Immunohistochemical, and Molecular study of 21 Cases Supporting an Emerging Heterogeneous Novel Group Spanning a Wide Clinical and Morphological Spectrum

Lin Yu¹, I Weng Lao¹, Meng Sun¹, Lu Zhao¹, Qianming Bai², Yao Qianlan³, Xiao-Yan Zhou², Jian Wang²
¹Fudan University Shanghai Cancer Center, Fudan University, Shanghai, China, ²Fudan University Shanghai Cancer Center, Shanghai, China, ³Fudan University Shanghai Cancer Center, Shanghai Medical College, Fudan University, Shanghai, China

Disclosures: Lin Yu: None; I Weng Lao: None; Meng Sun: None; Lu Zhao: None; Qianming Bai: None; Yao Qianlan: None

Background: Recently, NTRK-rearranged spindle cell neoplasm (outside infantile fibrosarcoma) as an emerging group molecularly defined has been included into the 5th edition WHO classification of soft tissue and bone tumors; however, its clinical and histologic features are yet to be completely understood. Herein, we present 21 cases of NTRK1 rearranged mesenchymal tumors to further characterize this newly nominated neoplasm and expand its clinical and pathological spectrum.

Design: The clinicopathological data of 21 cases of NTRK1 rearranged mesenchymal tumor were collected; morphological observation, immunohistochemical staining, interphase fluorescence in situ hybridization (FISH) and high-throughput DNA and RNA sequencing were performed, and the literatures were also reviewed.

Results: There were 13 males and 8 females with 15 pediatrics and 6 adults (range 4 mo to 44 y, mean 11.6 y, median 5 y). The most common tumor site was the extremity (n = 11), followed by head and neck (n = 6), trunk (n = 2), pelvic cavity(n = 1), and small intestine (n = 1), respectively. The mean tumor size was 4.2cm (range 1.0 to 16.0 cm). Histologically, 16 tumors displayed low grade features, with 9 showing lipofibromatosis-like neural tumor (LPF-NT) and 7 showing solid proliferation of spindle cells merged with variable amounts of collagen fibers; 2 displayed high grade features, with 1 each showing malignant peripheral nerve sheath tumor-like and infantile fibrosarcoma-like, respectively; and the remaining 3 exhibited intermediate grade, with 1 showing epithelioid

morphology. Fourteen cases showed dual expression of S100 and CD34, whereas the remaining 7 had a nonspecific immunoprofile. TrkA was positive in all tumors with concurrent pan-Trk staining in 10 tested cases. Fluorescence in situ hybridization (FISH) revealed NTRK1 rearrangement in all 21 tumors. Targeted DNA and/or RNA sequencing in 14 tumors identified LMNA-NTRK1(n=9), TPM3-NTRK1(n=2), TPR-NTRK1(n=1), CHTOP-NTRK1(n=1) and MYH10-NTRK1(n=1) fusions. The tumors clinically ranged from benign, locally aggressive to highly malignant. Of 20 patients with follow-up (range 6-92 mo, mean 28.4 mo, median 19.5 mo), 8 had no local recurrence and metastasis (range 6-35 mo, mean 21.3, median 27 mo), 9 experienced local recurrence (range 1-48 mo, mean 17.1mo, median 12 mo) , whereas 4 developed distant metastasis (range 3-13 mo, mean 8.3 mo, median 8.5 mo); 8 patients were alive with disease, and 12 were free of disease.

TABLE 1. Clinicopathological Features of 21 Cases of NTRK1 Rearranged Mesenchymal Tumor

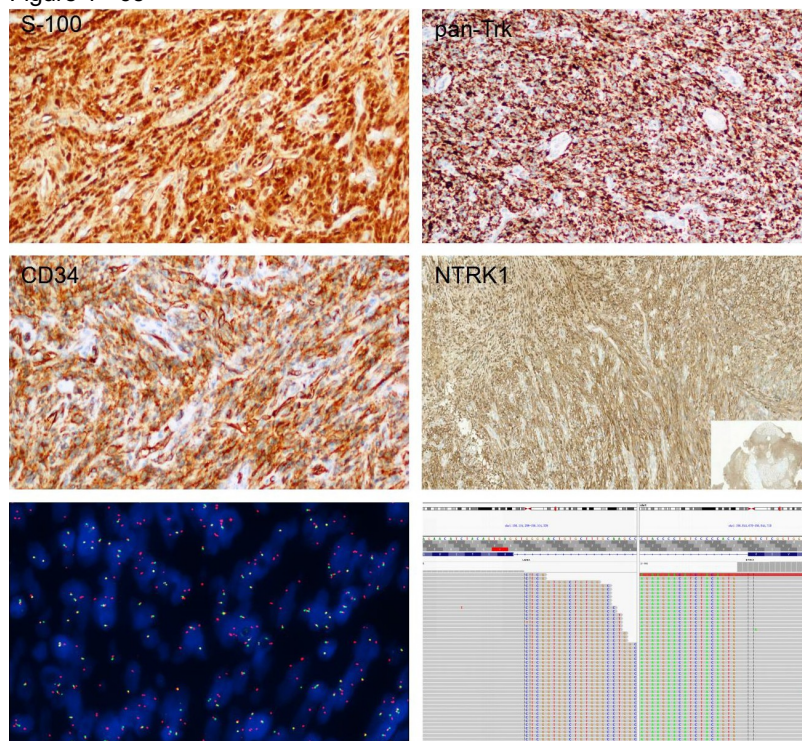
Case #	Sex	Age	Location	Tumor Size (cm)	Signs and Symptoms	Duration	Histological Grade	Mitosis /10 HPF	Referring Diagnosis	Treatment/Effect	Recurrence (mo)	Metastasis (mo)	Outcome (mo)	Disease Status
1	F	1y	Back	1.5	Slowly enlarging painless mass arising from congenital erythema	1 year	LG	1	LG fibroblastic tumor	Local excision	No	No	NED	13 13
2	M	1y	Scalp	3	Slowly enlarging painless mass arising from congenital erythema	1 year	LG	3	Spindle cell tumor, unclassified	Local excision	No	No	NED	29 29
3	F	4y	Thigh	3	Palpable non-tender mass	1 week	IG	2	ERMS	Local excision+radio+chemo(vincristine and adriamycin)/PD, larotrectinib(4 mo)/PR of lung metastatic lesions	No	Lung and inguinal lymph node,4	AW D	4 8
4	M	4y	Upper arm	8	Palpable non-tender mass	2 months	LG		Fibroma	Debulking, wide excision (after local recurrence)	1 x, 26	No	NED	26 37
5	M	5y	Infrapatellar fossa	3	Palpable non-tender mass	3 weeks	LG	0	LG spindle cell sarcoma	Local excision	No	No	NED	11 11
6	F	5y	Neck	3	Gradually enlarging painless mass arising from congenital erythema	10 months	LG	1	Neurofibroma, DFSP, lipomatous neoplasm	Local excision	No	No	NED	35 35
7	F	7y	Buttock	4	Slowly enlarging painless mass arising from congenital erythema	7 years	LG	4	Spindle cell tumor, unclassified	Wide excision	No	No	NED	28 28
8	M	9y	Pelvic cavity	16	Abdominal distension	1 week	LG	24	LG fibroblastic tumor	Local excision+chemo(vincristine and adriamycin, 3 cycles)/PD, anlotinib(3 mo)/PD, apatinib(3 mo)/PD	1 x, 5	Vertebra,13	AW D	5 16
9	F	2y	Popliteal fossa	3	Slowly enlarging painless mass	2 years	LG	0	Atypical spindle cell/pleomorphic lipomatoid tumor	Local excision	NA	NA	NA	N N A A
10	F	2y	Thigh	1.4, 1.5	Slowly enlarging painless mass arising from congenital erythema	24 years	LG	1	LPT-NT	Local excision	No	No	NED	27 27
11	M	3y	Upper arm	3	Palpable non-tender mass	6 months	LG	3	NA	Wide excision	No	No	NED	6 6

ABSTRACTS | BONE AND SOFT TISSUE PATHOLOGY

12	M	4y	Small intestine	9	Hematochezia	2 weeks	HG	24	LG spindle cell sarcoma	Local excision+anlotinib (3 mo)/PD	No	Abdominopelvic cavity, 3	AW 3 10 D
13	M	4y	Knee	5.5	Palpable non-tender mass	5 months	LG	4	SFT	Local excision	No	Lung,13	AW 13 15 D
14	M	8y	Hand back	2.5	Palpable non-tender mass	1 year	LG	2	SFT	Debulking, wide excision (after local recurrence)	1x, 12	No	NED 12 56
15	M	6y	Superciliary arch	2.6	Slowly enlarging painless mass arising from congenital erythema	2 years	LG	1	DFSP	Debulking, wide excision (after local recurrence)	1x, 7	No	NED 7 19
16	M	4y	Leg	1.6	Slowly enlarging painless mass arising from congenital erythema	4 years	LG	4	IMT,DFSP	Local excision	1x, 12	No	AW 12 24 D
17	F	1y	Knee	6	Gradually enlarging painless mass arising from congenital erythema	1 year	HG	42	IFS	Local excision, chemo(vincristine and adriamycin, 3 cycles) /SD (after local recurrence)	1x, 1	No	AW 1 15 D
18	M	37y	Neck	8	Palpable non-tender mass	NA	LG	4	LG MPNST	Local excision	1x, 27	No	AW 27 27 D
19	M	4y	Hand back	3.5	Palpable non-tender mass	4 months	LG	1	Lipofibromatosis	Debulking, local excision (after local recurrence)	2x, 48,72	No	AW 48 92 D
20	F	20y	Back	2.8	Palpable non-tender mass	1 year	IG	9	MPNST	Local excision, wide excision +/- radio (after local recurrence)	6x, 16,22,40,55,68,71	No	NED 16 78
21	M	2y	Upper lip	1	Slowly enlarging painless mass arising from congenital erythema		LG	0	Spindle cell tumor,unclassified	Biopsy+wide excision	No	No	NED 31 31

AWD indicates alive with disease;DFSP,dermatofibrosarcoma protuberans;DOD, dead of disease; DFS, disease-free survival;ERMS,embryonal rhabdomyosarcoma;HG,high grade;IG,intermediate grade;IFS,infantile fibrosarcoma;IMT,inflammatory myofibroblastoma;LG,low-grade;LPT-NT,lipofibromatosis-like neural tumor;MPNST,malignant peripheral nerve sheath tumor;NA,not available;NA,not available;NED,no evidence of disease; OS,overall survival; PR,partial response; PD,progressvie disease; SFT,solitary fibrous tumor;SD,stable disease.

Figure 1 - 65



Conclusions: NTRK1 rearranged mesenchymal tumor represents a novel group of heterogeneous tumors spanning a wide spectrum of morphology and clinical outcome. The early and precise recognition of these tumors is of increasing clinical importance for targeted therapy of Trk inhibitors.